

Evaluation and Modeling of the Effect of Novel Pad Grooves on Copper CMP

Daniel Rosales-Yeomans

The University of Arizona, Tucson AZ USA

January 25, 2007



**NSF/SRC ERC for Environmentally Benign
Semiconductor Manufacturing**

Grooved Pads in CMP

Grooves in CMP pads:

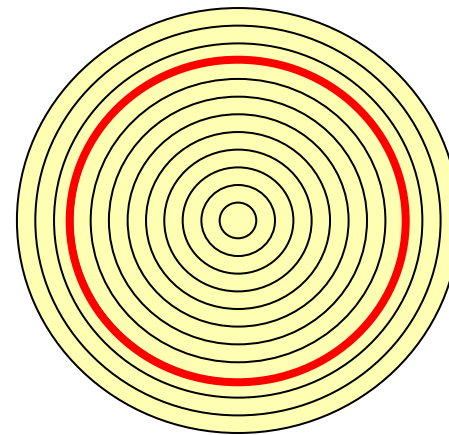
Prevent hydroplaning

Ensure uniform slurry distribution across the pad and into the wafer-pad interface

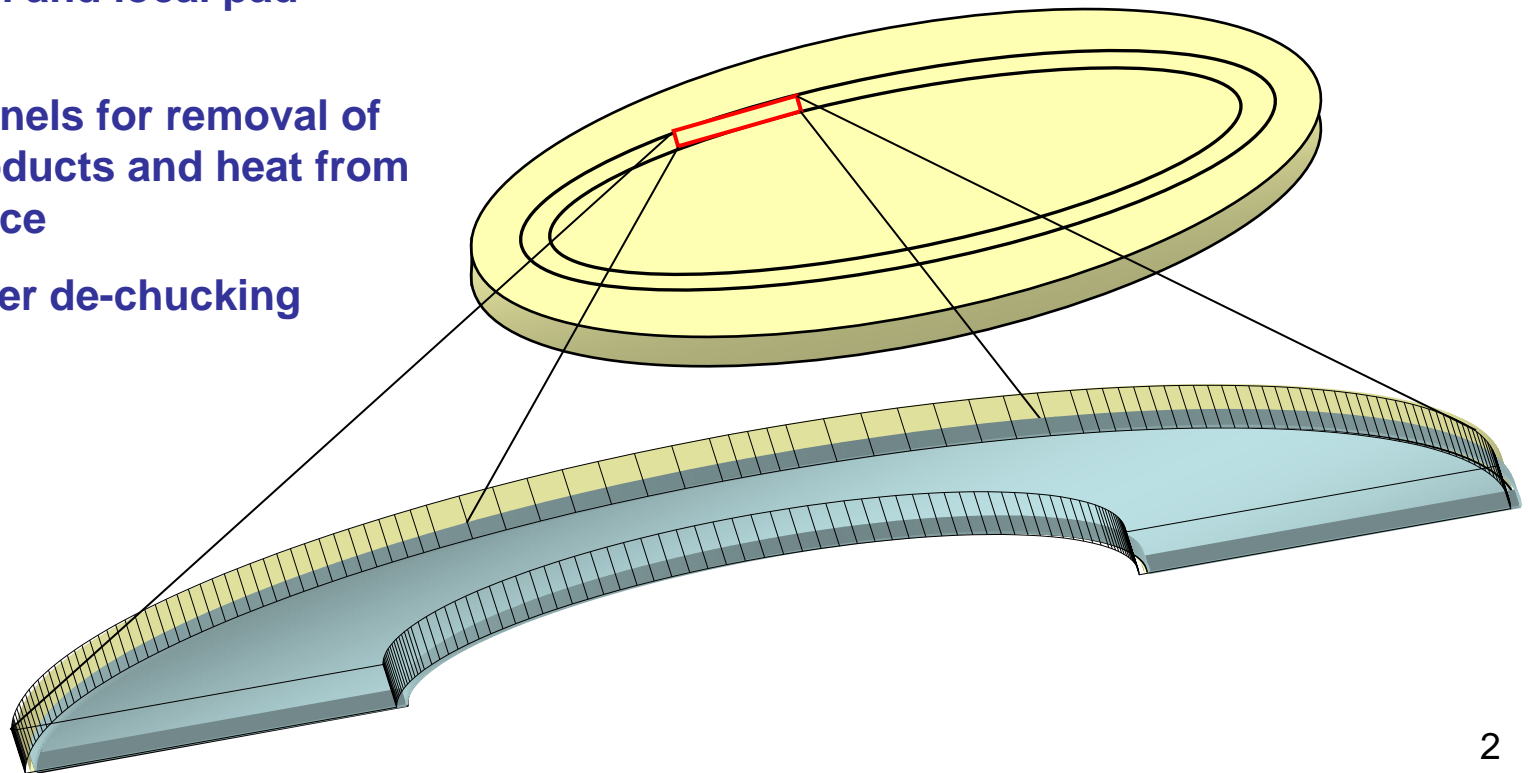
Adjust overall and local pad stiffness

Provide channels for removal of polish by-products and heat from the pad surface

Allow for wafer de-chucking



Concentric Grooves

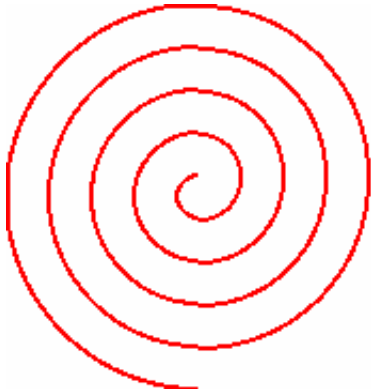


Outline

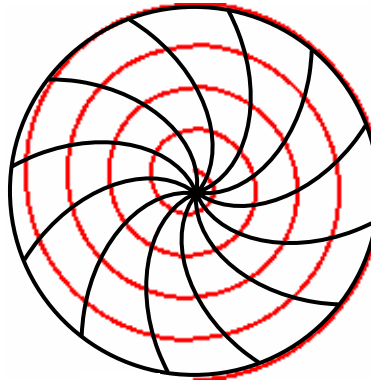
- **Grooves Design (and experimental conditions)**
 - Logarithmic-Spiral
 - Concentric Slanted
- **Experimental Results**
 - Logarithmic-Spiral
 - RR and average pad temperature
 - Average COF
 - Statistical comparison among different pad grooves
 - Concentric Slanted
 - RR and average pad temperature
 - Average COF
 - Statistical comparison among different pad grooves
- **3-Step Model Development**
 - Driving Force
 - Passive Film Formation and Dissolution
- **3-Step Model Evaluation and Application**

Logarithmic-Spiral Grooves

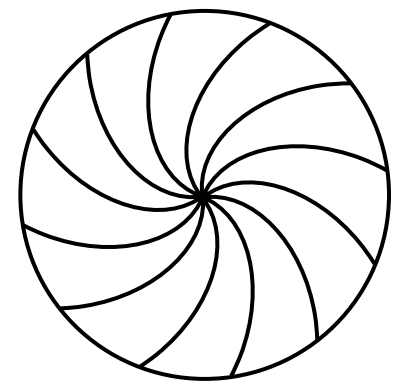
Spiral (+)



Logarithmic (+) Spiral (-)



Logarithmic (-)



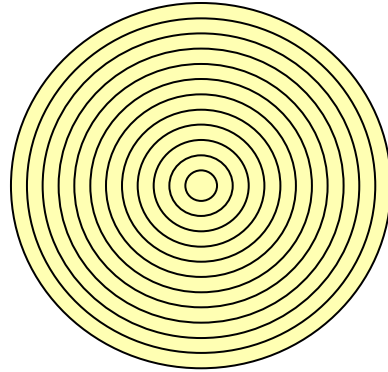
Basic Idea ...

Positive Log. and Spiral Grooves Transport fresh slurry into the pad – wafer interface

Negative Log. and Spiral Grooves Discharge spent slurry and by – products away from the pad – wafer interface

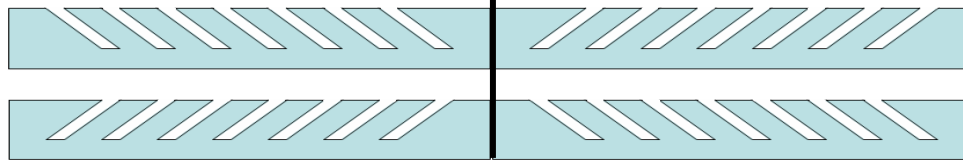
Wafer and pad (i.e grooves) rotate in the **counter-clockwise** direction

Concentric Slanted Grooves



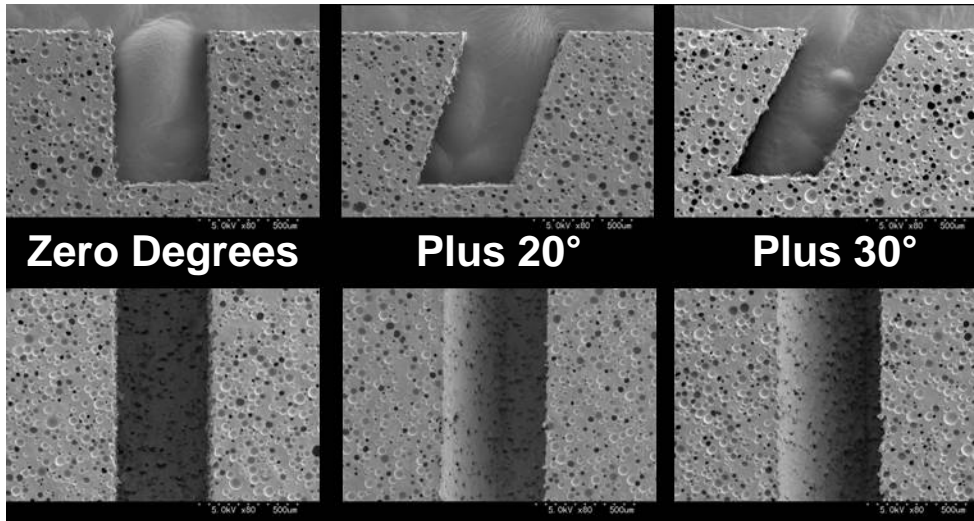
Wafer and pad (i.e grooves) rotate in the **counter-clockwise** direction

Center of the pad



Positive Direction

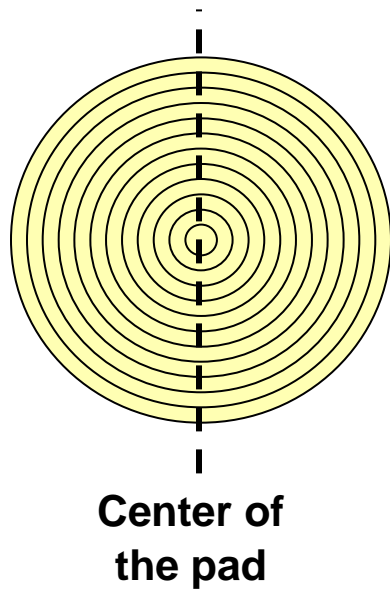
Negative Direction



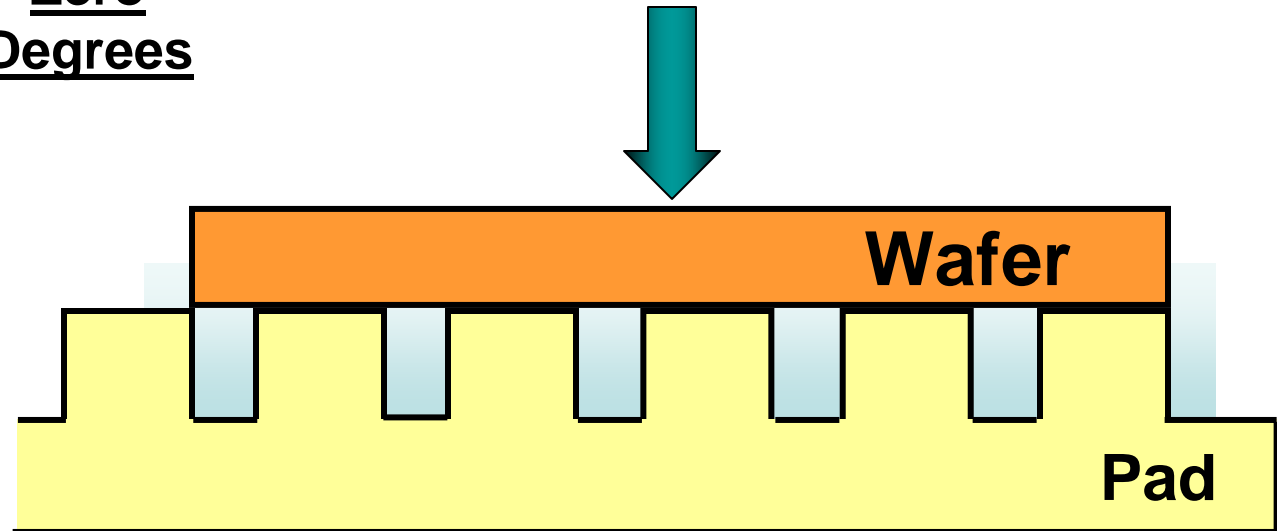
Side View

Top View

Concentric Slanted Grooves

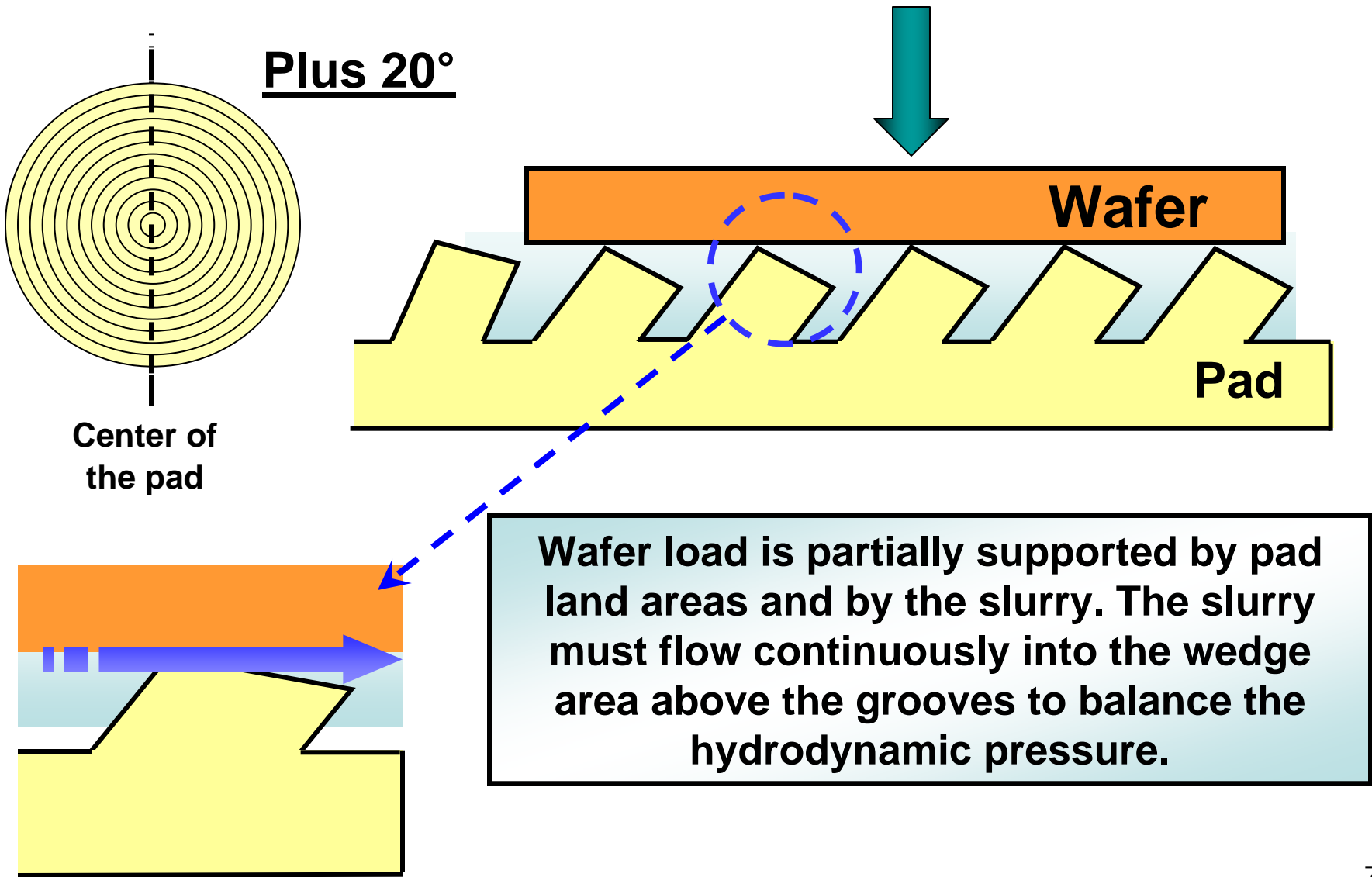


Zero
Degrees



Wafer load is mostly supported by pad land areas. Slurry is confined to the inside of the grooves.

Concentric Slanted Grooves



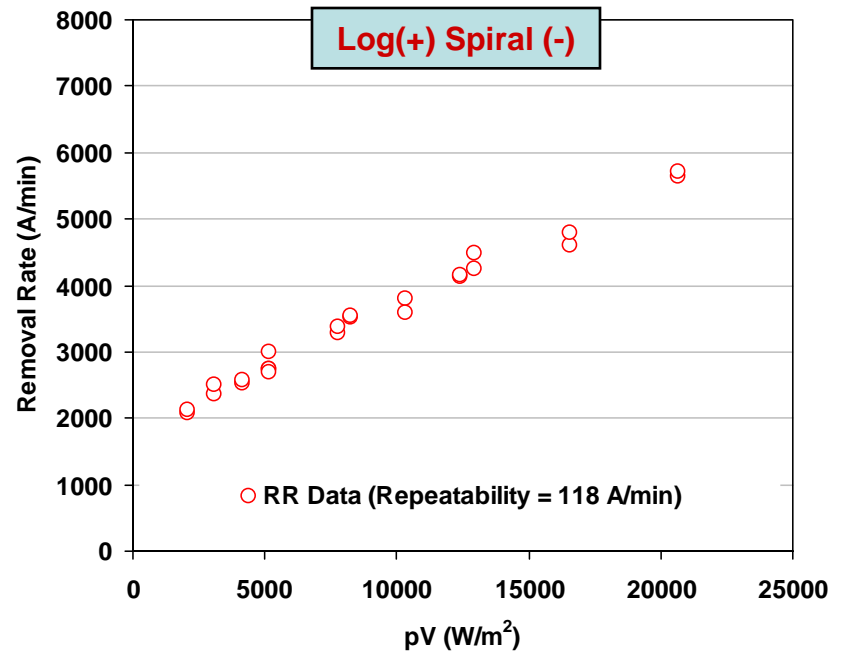
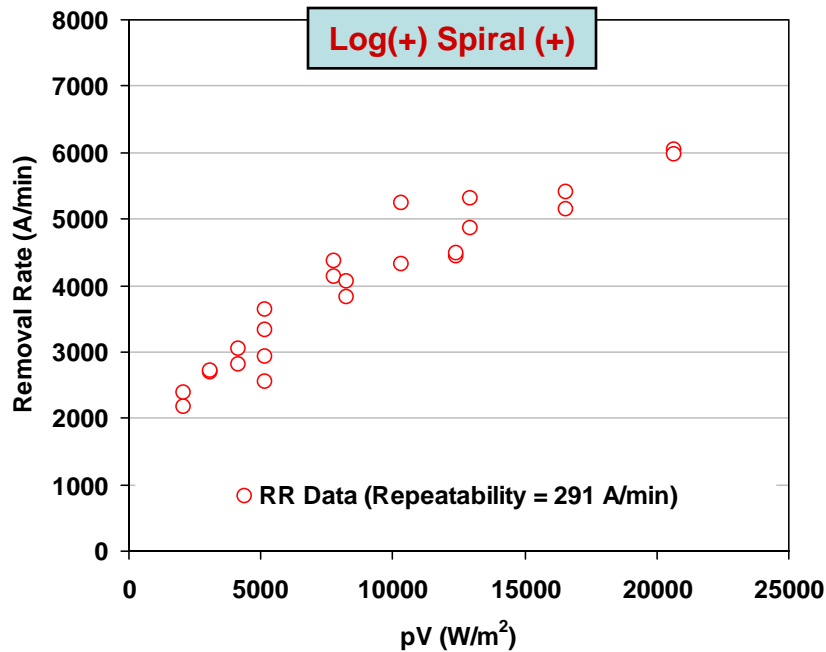
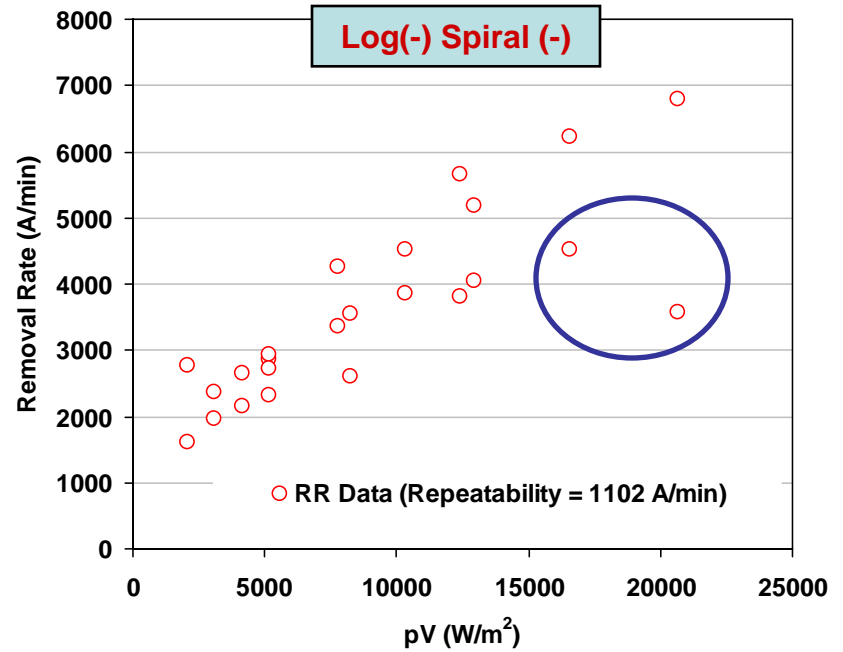
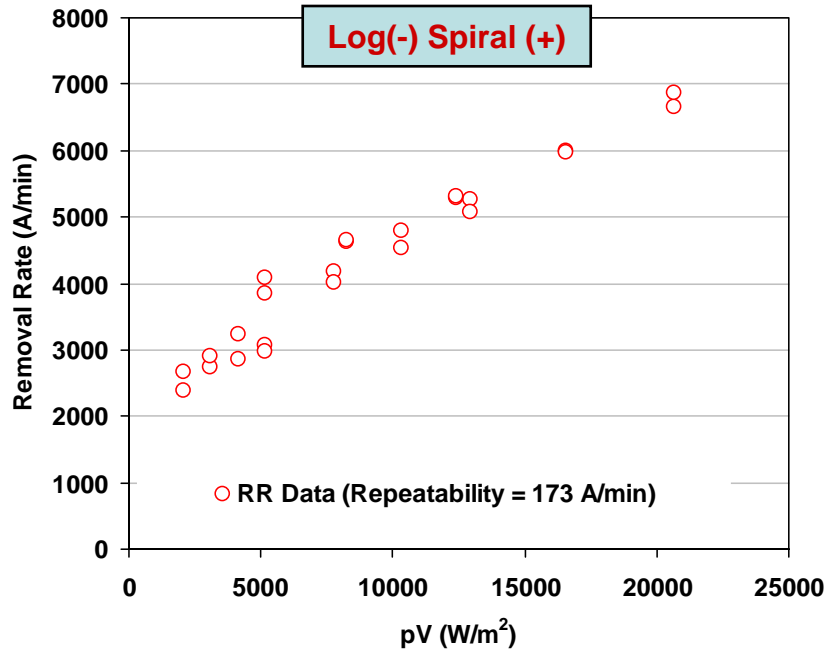
Experimental Conditions

- Constants:
 - **Conditioning**
 - 100 grit diamond disc (TBW)
 - 30 min with UPW at 30 rpm disc speed and 20 per min sweep frequency
 - **Break-in**
 - 5 dummy Discs (Cu) with Fujimi PL-7102
 - **Slurry**
 - Fujimi PL-7102
 - 220 cc per minute
 - **Wafers**
 - 200-mm Cu wafers
- Variables:
 - **Relative pad-wafer velocity (m/s)**
 - 0.30
 - 0.75
 - 1.20
 - **Wafer pressure (PSI)**
 - 1.0 (6894 Pa)
 - 1.5 (10300 Pa)
 - 2.0 (13780 Pa)
 - 2.5 (17200 Pa)
 - **Pad groove design**
 - Concentric
 - Logarithmic Spiral
- Variables:
 - **Relative pad-wafer velocity (m/s)**
 - 0.30
 - 0.75
 - 1.20
 - **Wafer pressure (PSI)**
 - 1.0 (6894 Pa)
 - 2.0 (13780 Pa)
 - 3.0 (20,684 Pa)
 - **Pad groove design**
 - Concentric
 - Concentric Slanted

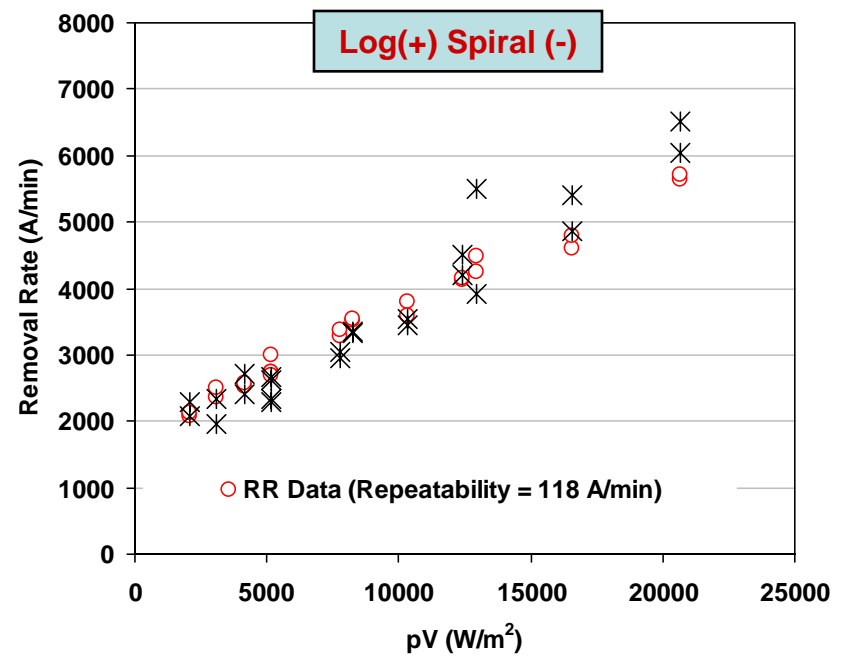
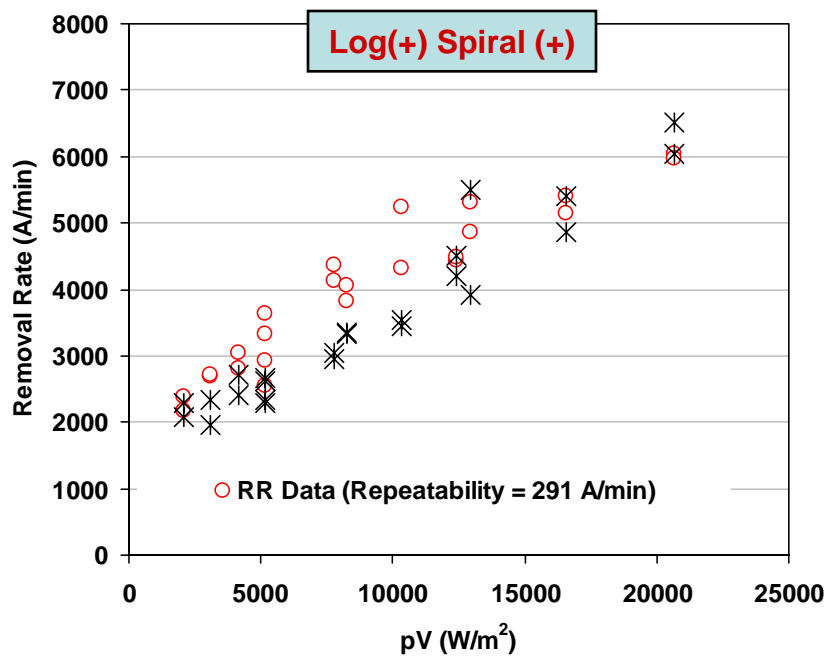
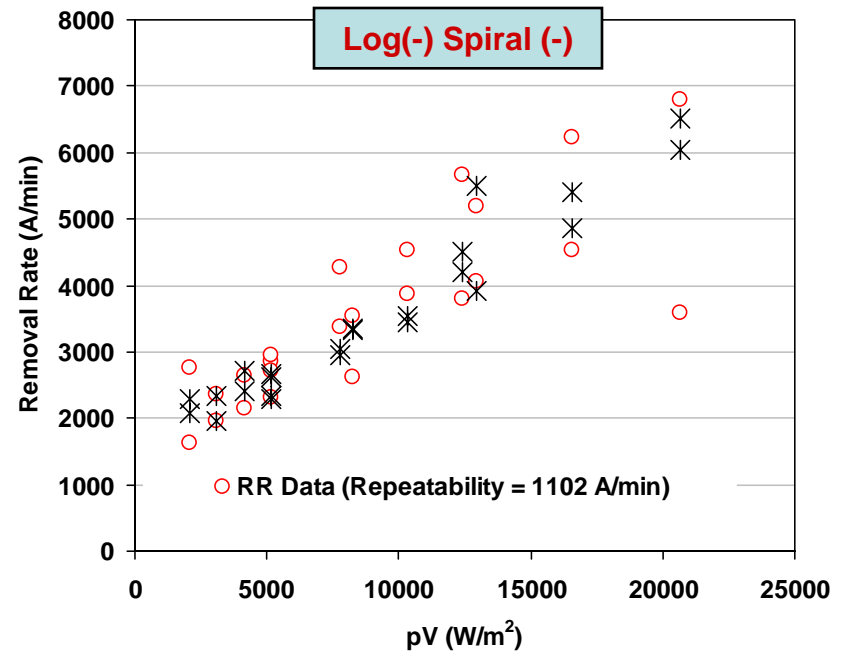
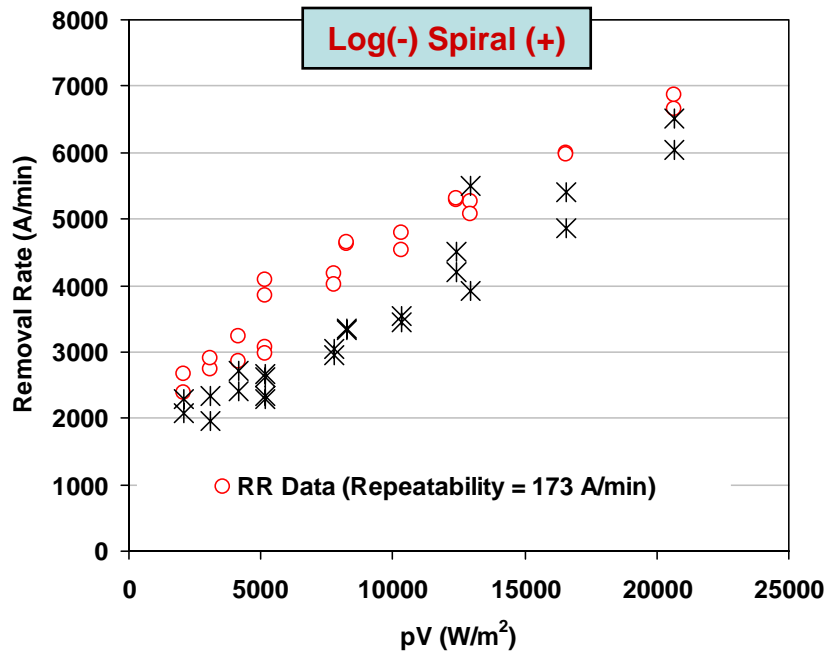
Outline

- **Grooves Design (and experimental conditions)**
 - **Logarithmic-Spiral**
 - **Concentric Slanted**
- **Experimental Results**
 - **Logarithmic-Spiral**
 - **RR and average pad temperature**
 - **Average COF**
 - **Statistical comparison among different pad grooves**
 - **Concentric Slanted**
 - **RR and average pad temperature**
 - **Average COF**
 - **Statistical comparison among different pad grooves**
- **3-Step Model Development**
 - **Driving Force**
 - **Passive Film Formation and Dissolution**
- **3-Step Model Evaluation and Application**

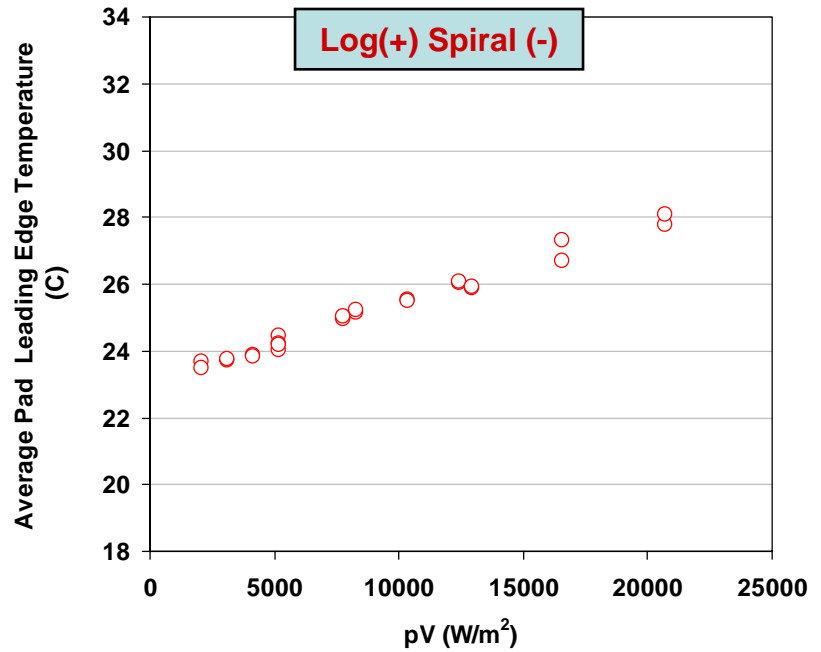
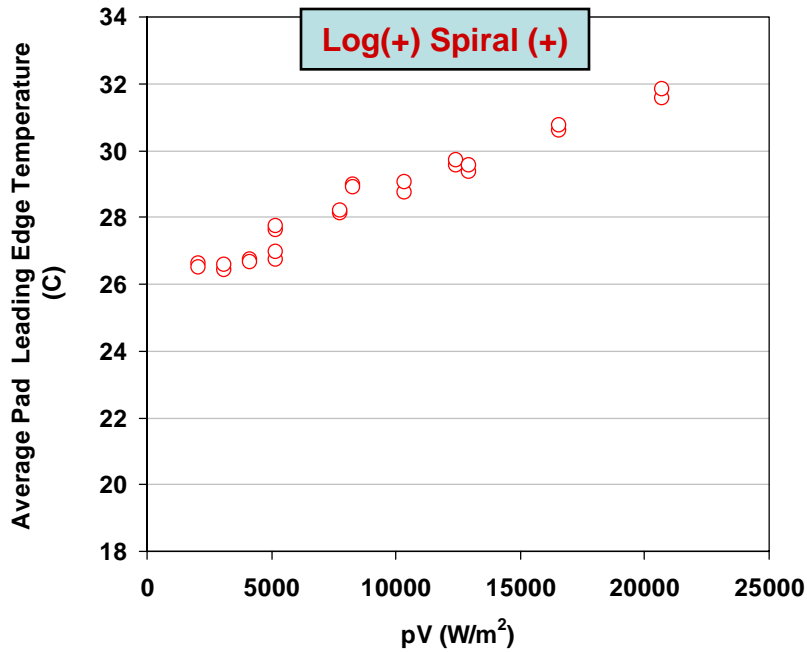
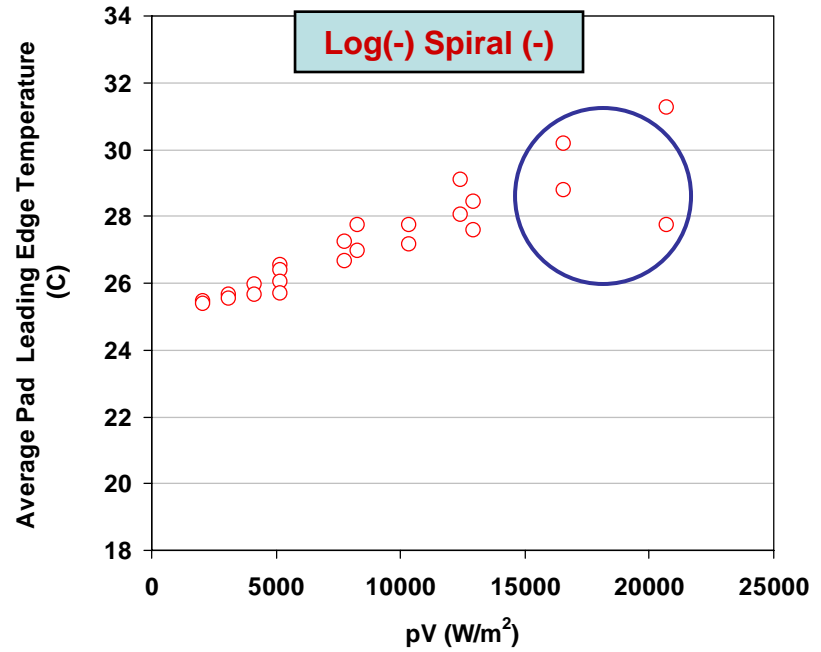
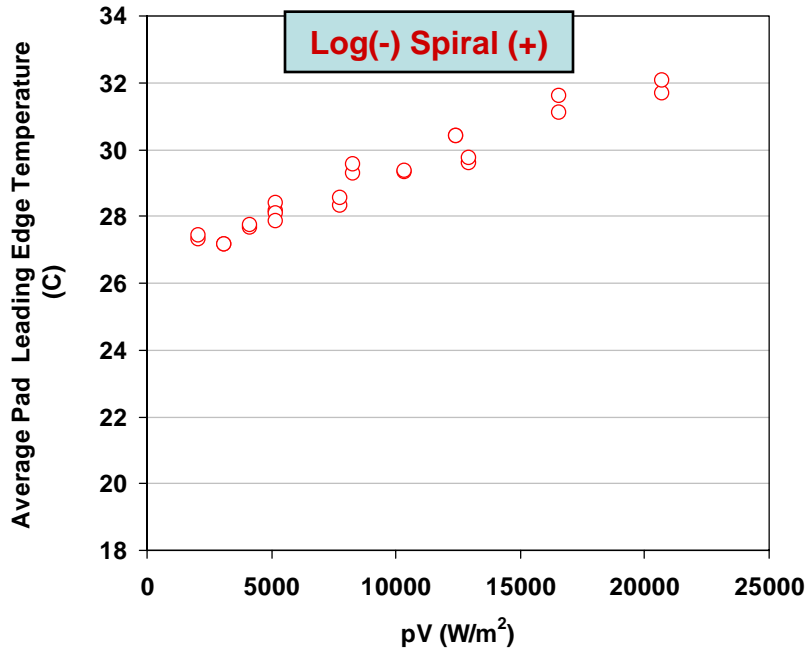
RR ... Logarithmic-Spiral Grooves



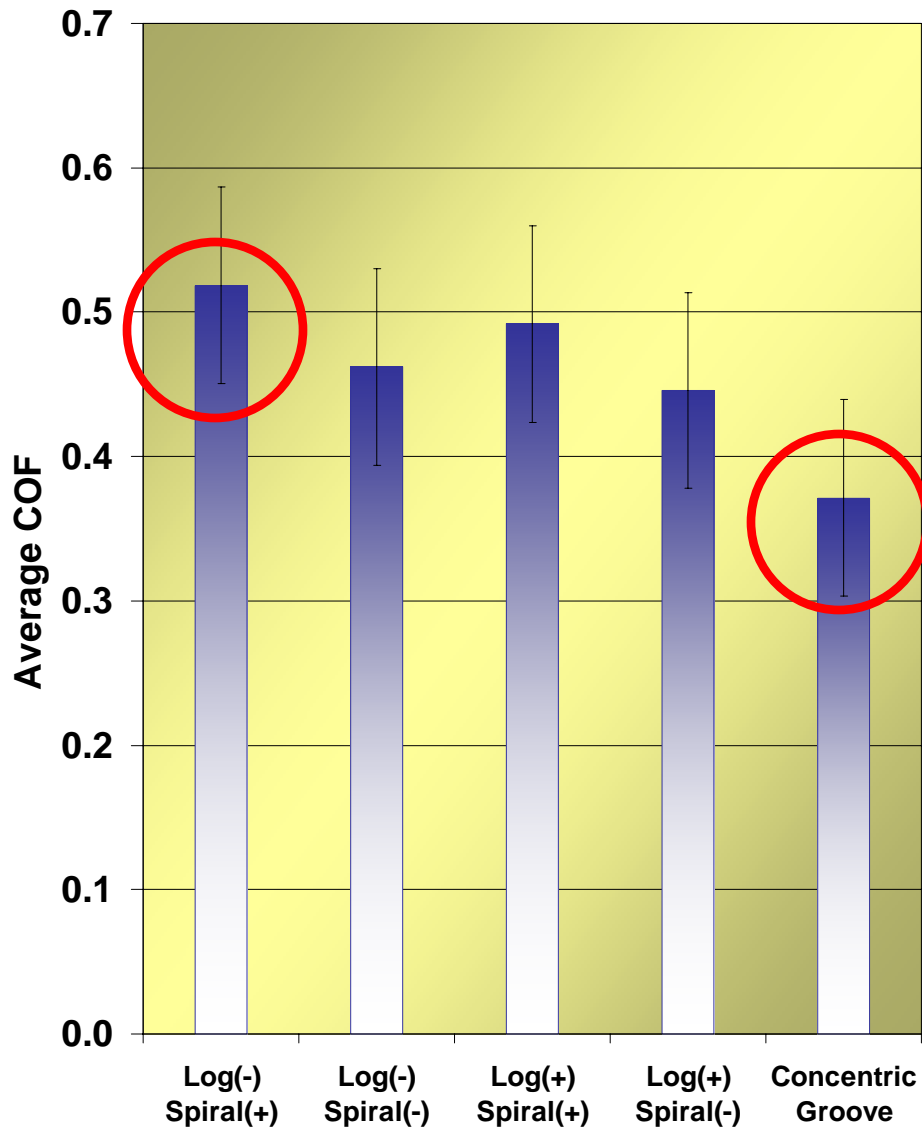
RR ... Logarithmic-Spiral Grooves



Average Pad Leading Edge Temperature ... Logarithmic-Spiral Grooves



Average COF and Shear Force... Logarithmic-Spiral Grooves



$$COF_{avg} = \frac{\overline{F}_{Shear}}{F_{Normal}}$$

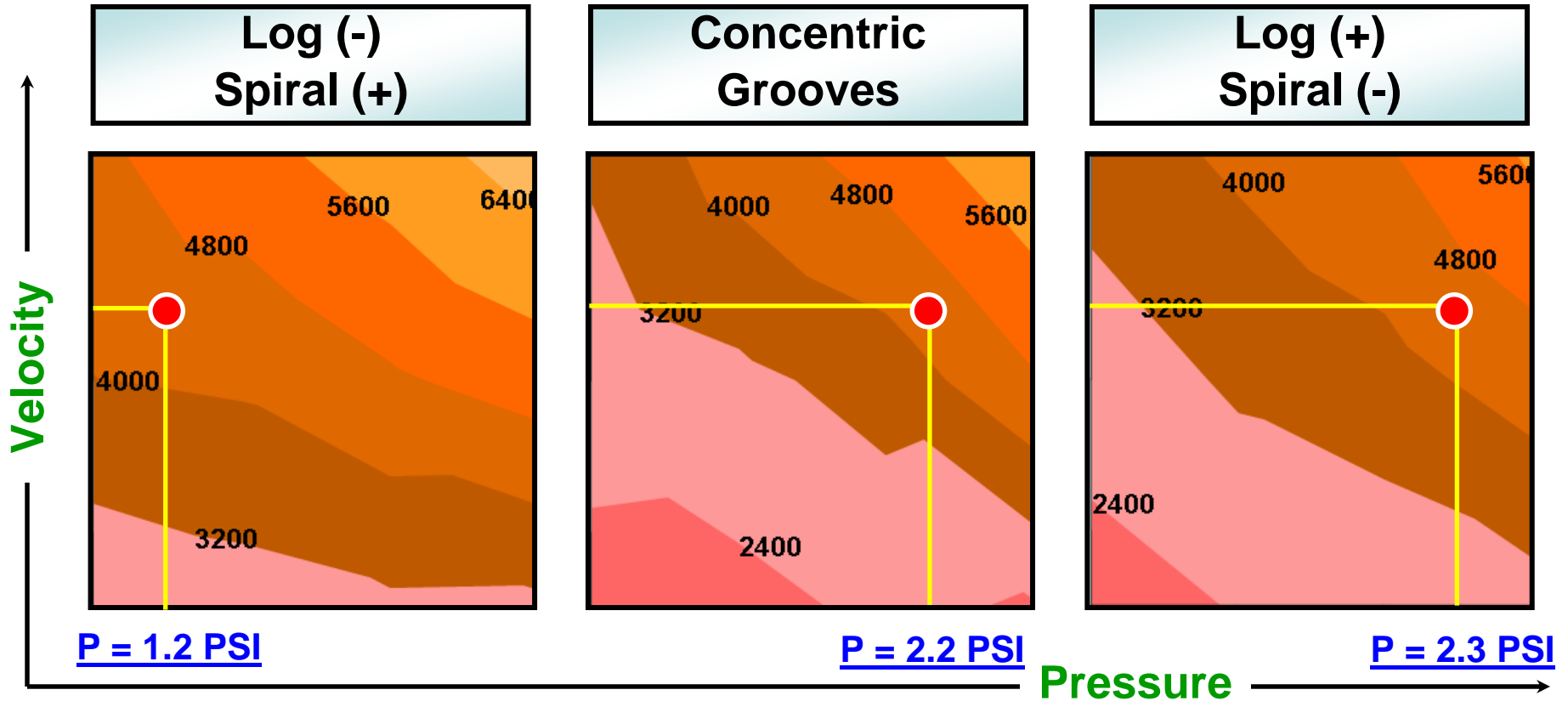
$$\overline{F}_{Shear} = COF_{avg} \times F_{Normal}$$

$$F_{Normal} \propto P_w$$

$$\overline{F}_{Shear} \propto COF_{avg} \cdot P_w$$

Log (-) Spiral (+)	Concentric Groove
$COF_{avg} = 0.52$	$COF_{avg} = 0.37$
$P_w = 1.0 \text{ psi}$	$P_w = 1.0 \text{ psi}$
$F_{shear} = 26 \text{ Lbf}$	$F_{shear} = 18.6 \text{ Lbf}$

Decoupling the effect of p and V on RR



At a given RR, the Log (-) Spiral (+) is less dependent on P (at constant V)

This is an advantage in polishing ULK materials where low pressures are required

In addition to increase pad life by reducing the applied pressure

Statistical Analysis (Wilcoxon Signed Rank Test) Logarithmic-Spiral Grooves

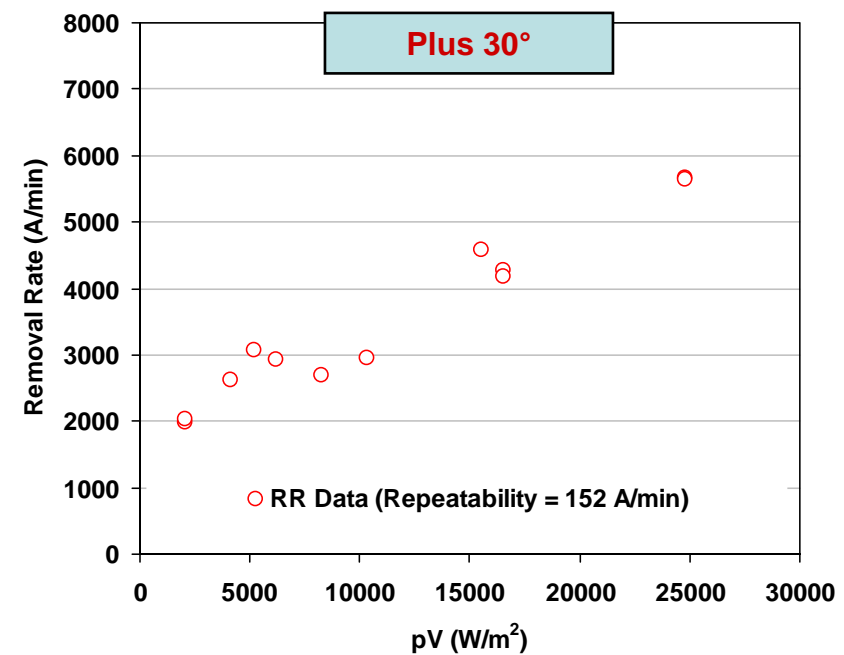
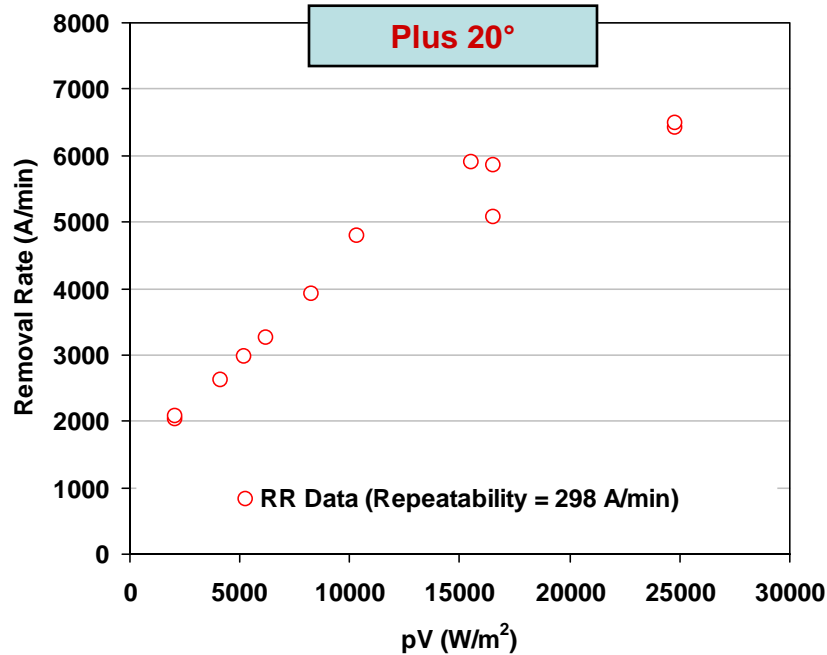
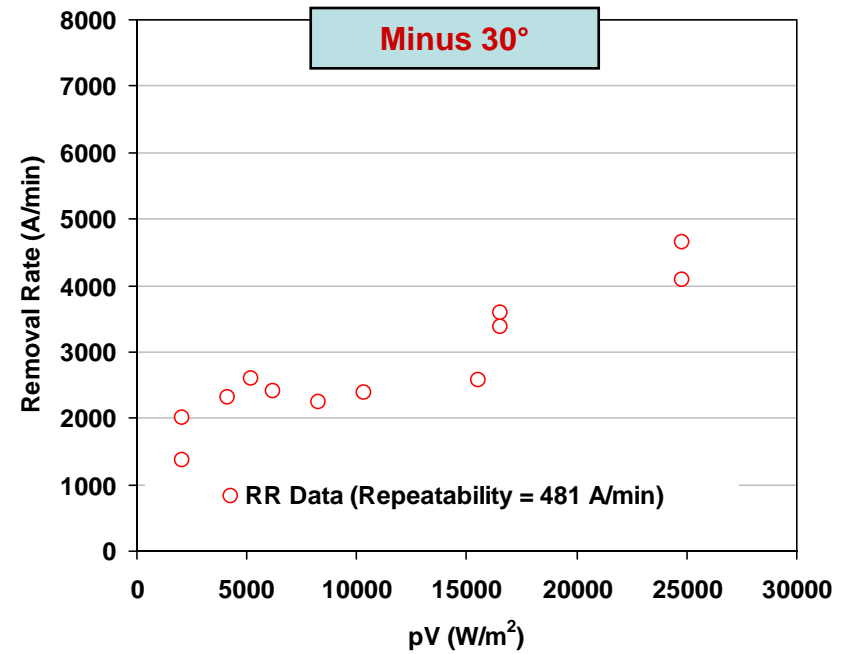
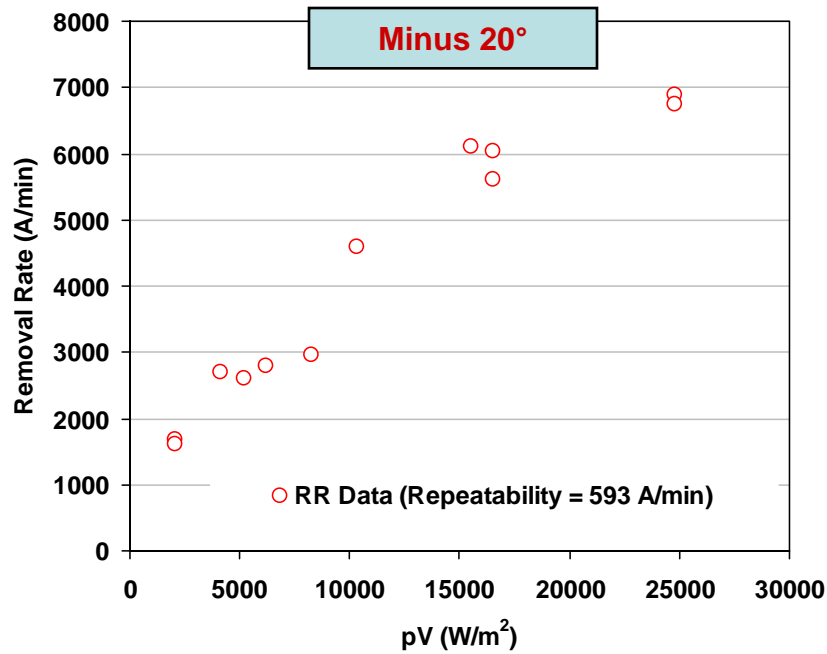
	Higher Rank = 1	Rank = 2	Lower Rank = 3
Removal Rate	Log (-) Spiral (+)	Log (-) Spiral (-) and Log (+) Spiral (+)	Log (+) Spiral (-) and Concentric Groove
Avg. Pad Leading Temperature	Log (-) Spiral (+) and Log (+) Spiral (+)	Log (-) Spiral (-)	Log (+) Spiral (-) and Concentric Groove

Results obtained with 95% confidence

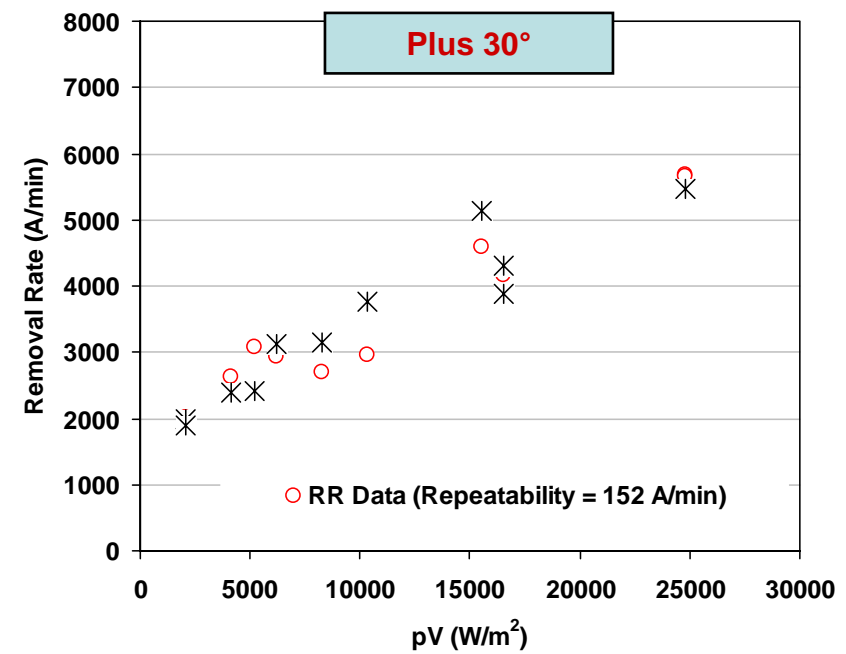
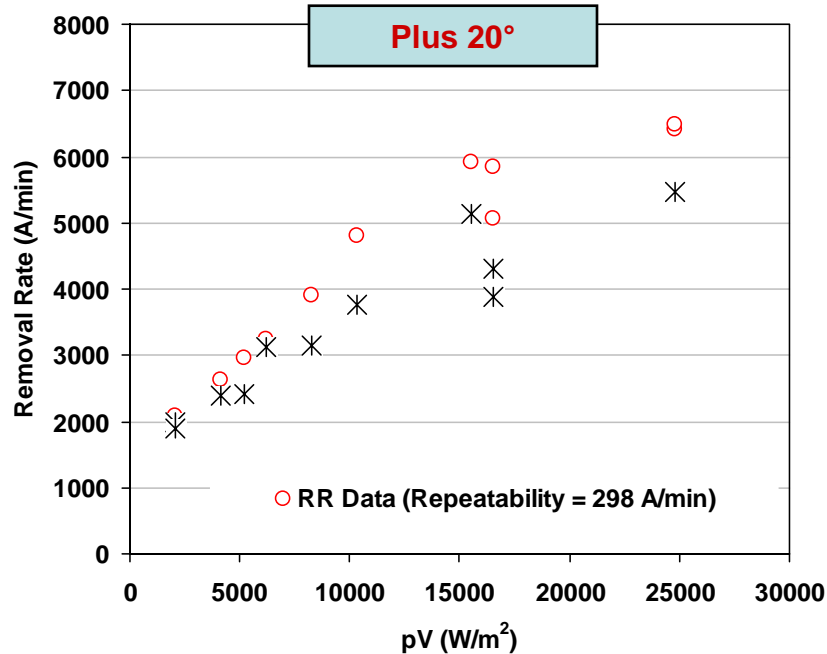
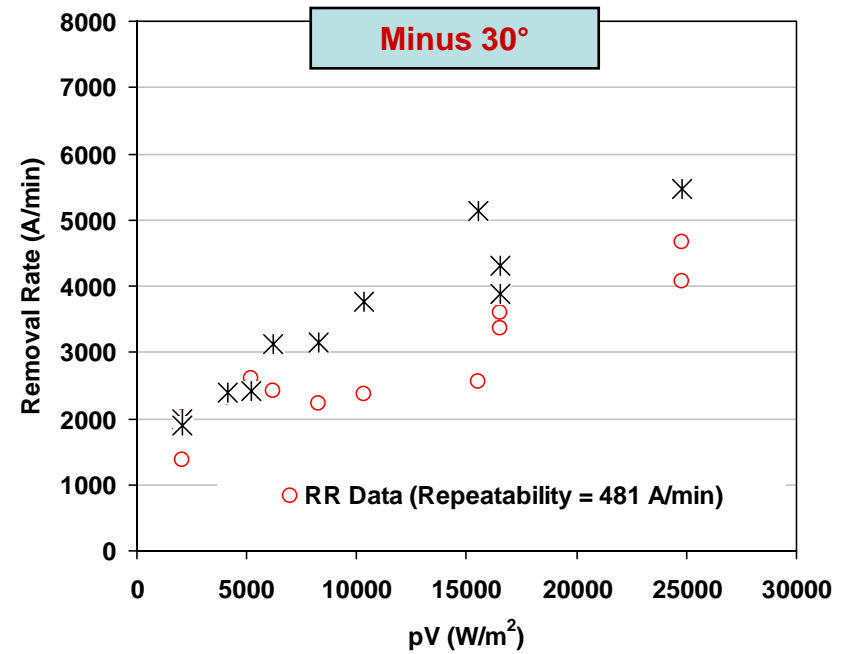
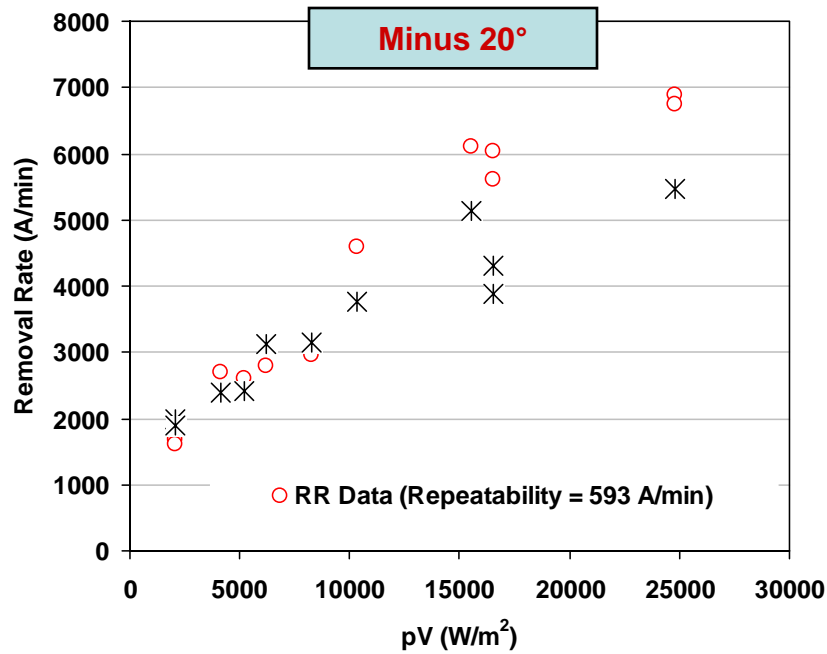
Outline

- **Grooves Design (and experimental conditions)**
 - **Logarithmic-Spiral**
 - **Concentric Slanted**
- **Experimental Results**
 - **Logarithmic-Spiral**
 - **RR and average pad temperature**
 - **Average COF**
 - **Statistical comparison among different pad grooves**
 - **Concentric Slanted**
 - **RR and average pad temperature**
 - **Average COF**
 - **Statistical comparison among different pad grooves**
- **3-Step Model Development**
 - **Driving Force**
 - **Passive Film Formation and Dissolution**
- **3-Step Model Evaluation and Application**

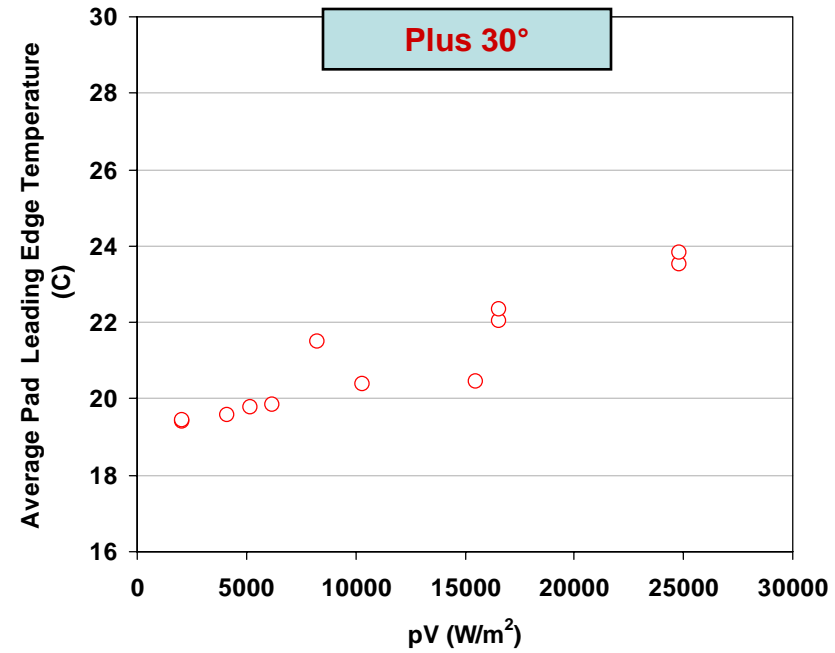
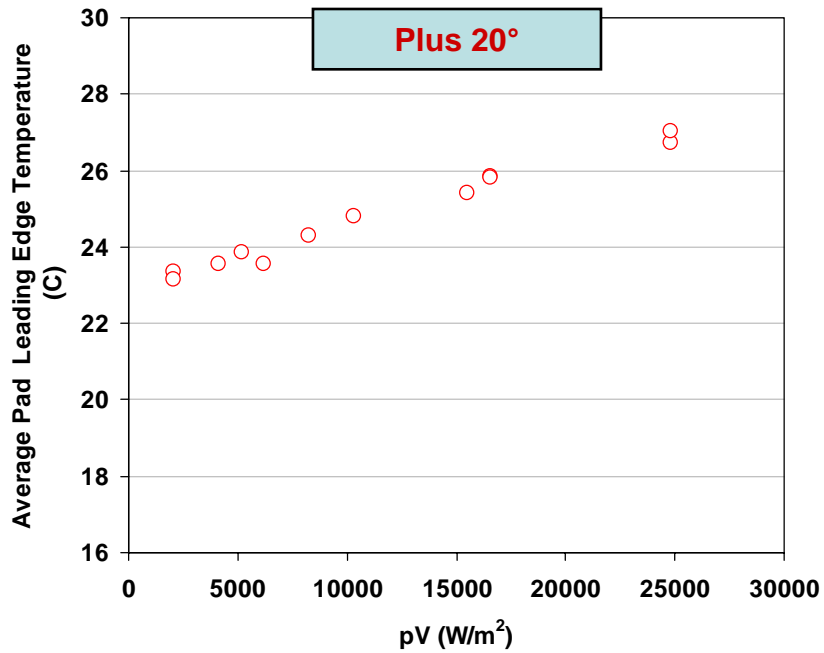
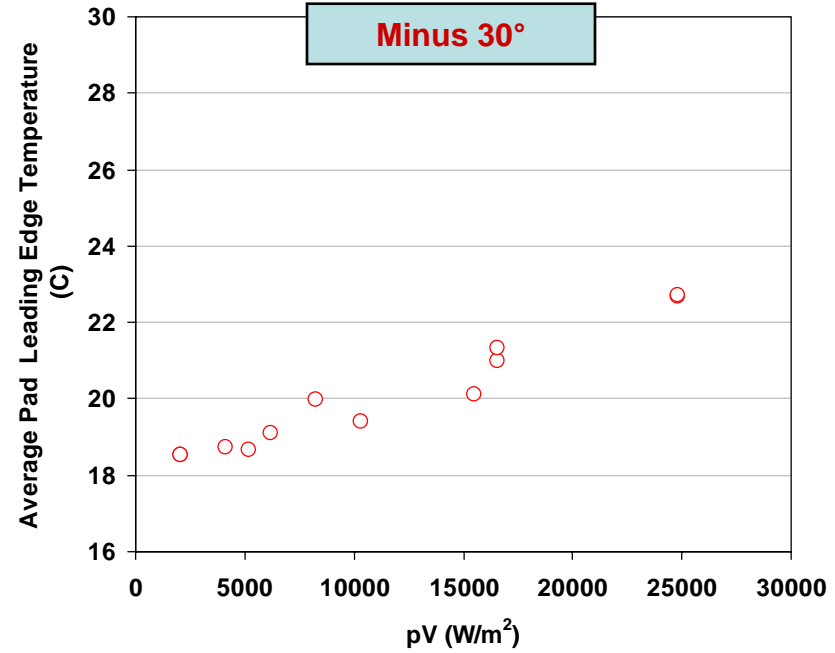
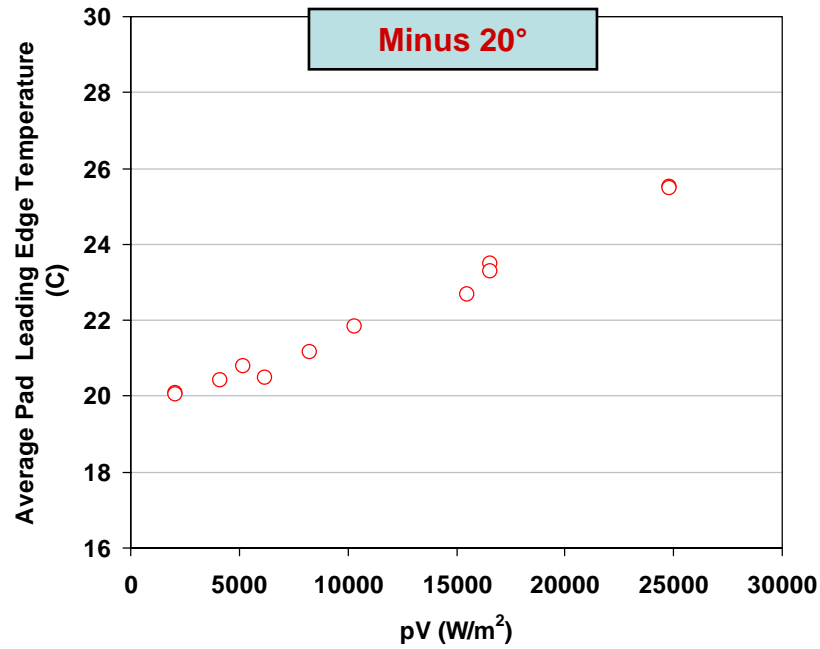
RR ... Slanted Grooves



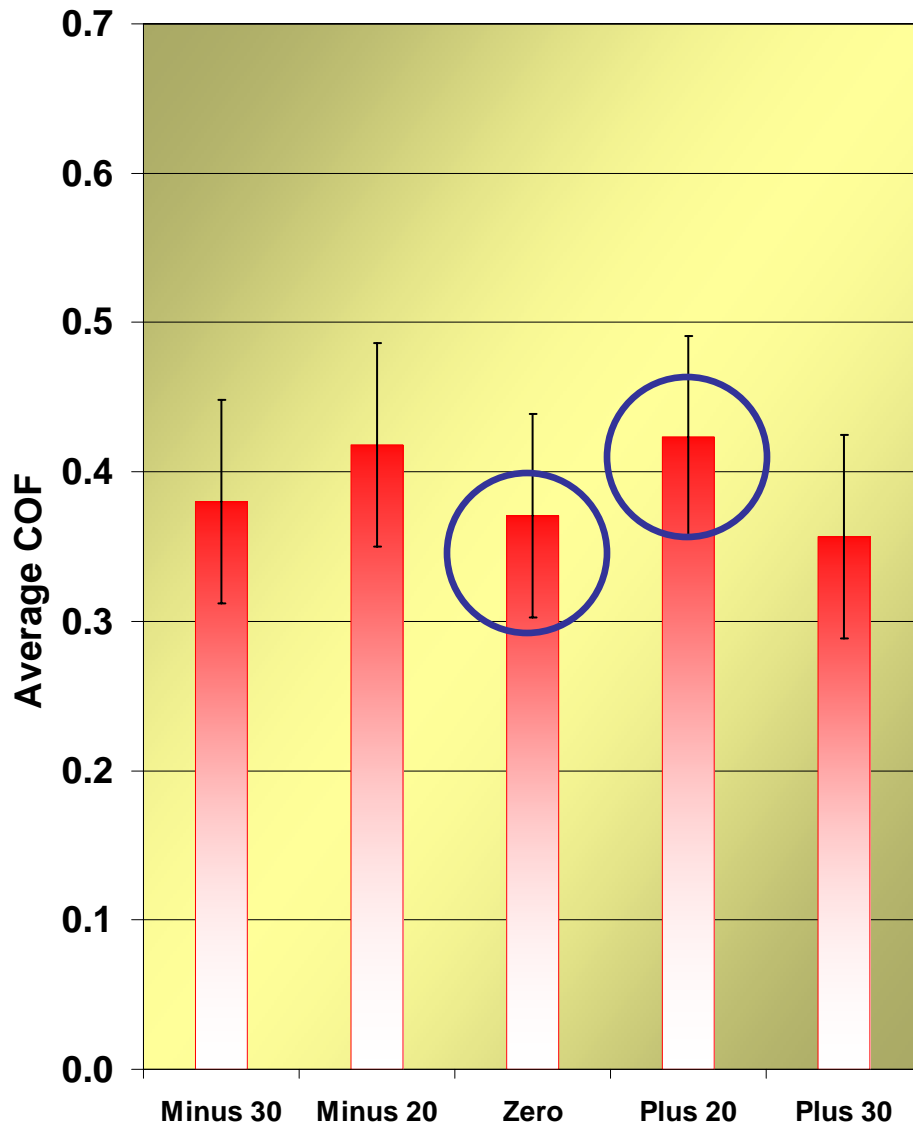
RR ... Slanted Grooves



Average Pad Leading Temperature ... Slanted Grooves



Average COF and Shear Force... Concentric Slanted Grooves



$$COF_{avg} = \frac{\overline{F}_{Shear}}{F_{Normal}}$$

$$\overline{F}_{Shear} = COF_{avg} \times F_{Normal}$$

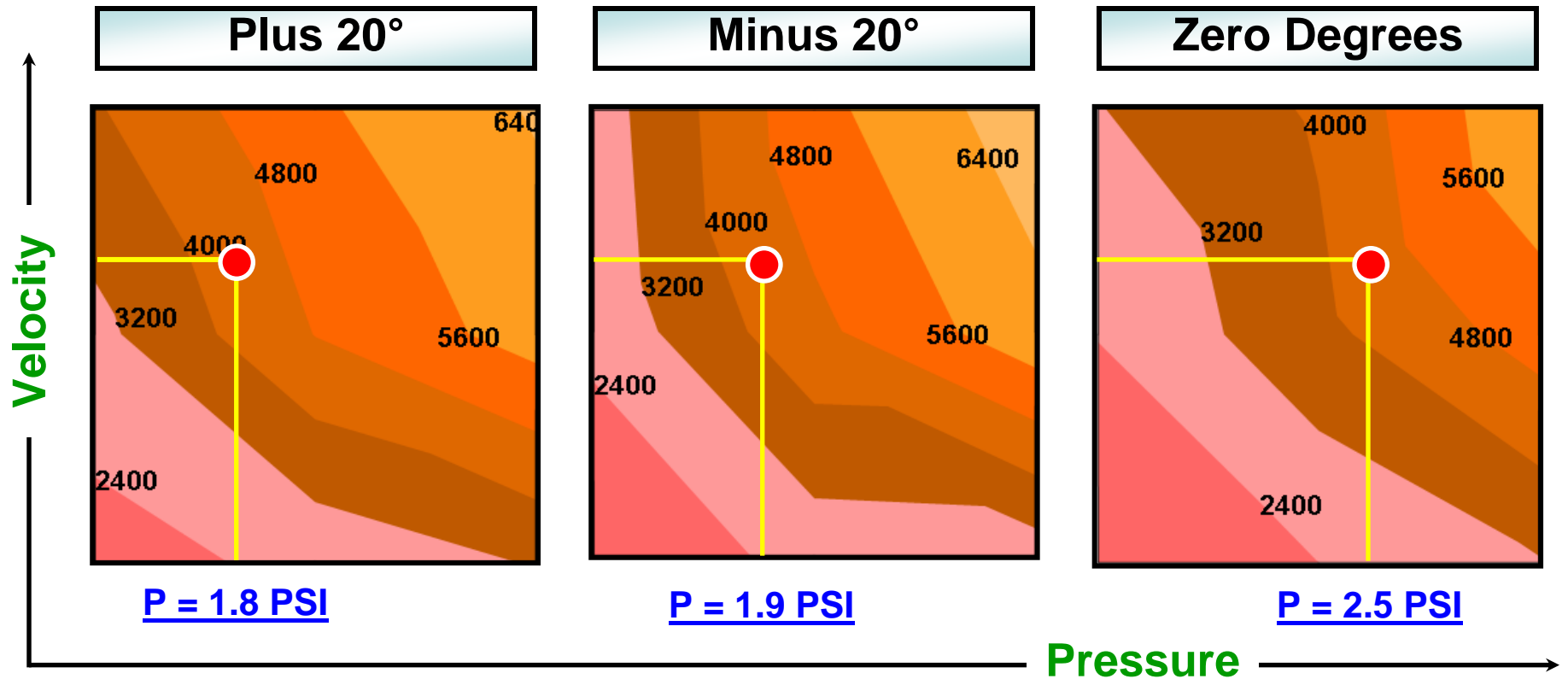
$$F_{Normal} \propto P_w$$

$$\overline{F}_{Shear} \propto COF_{avg} \cdot P_w$$

Plus 20°
 $COF_{avg} = 0.43$
 $P_w = 1.0 \text{ psi}$
 $F_{shear} = 22 \text{ Lbf}$

Zero degrees
 $COF_{avg} = 0.37$
 $P_w = 1.0 \text{ psi}$
 $F_{shear} = 18.5 \text{ Lbf}$

Decoupling the effect of P and V on RR



At a given RR, Plus 20° and Minus 20° are less dependent on P (at constant V)

This is an advantage in polishing ULK materials where low pressures are required

In addition to increase pad life by reducing the applied pressure

Statistical Analysis (Wilcoxon Signed Rank Test) Slanted Grooves

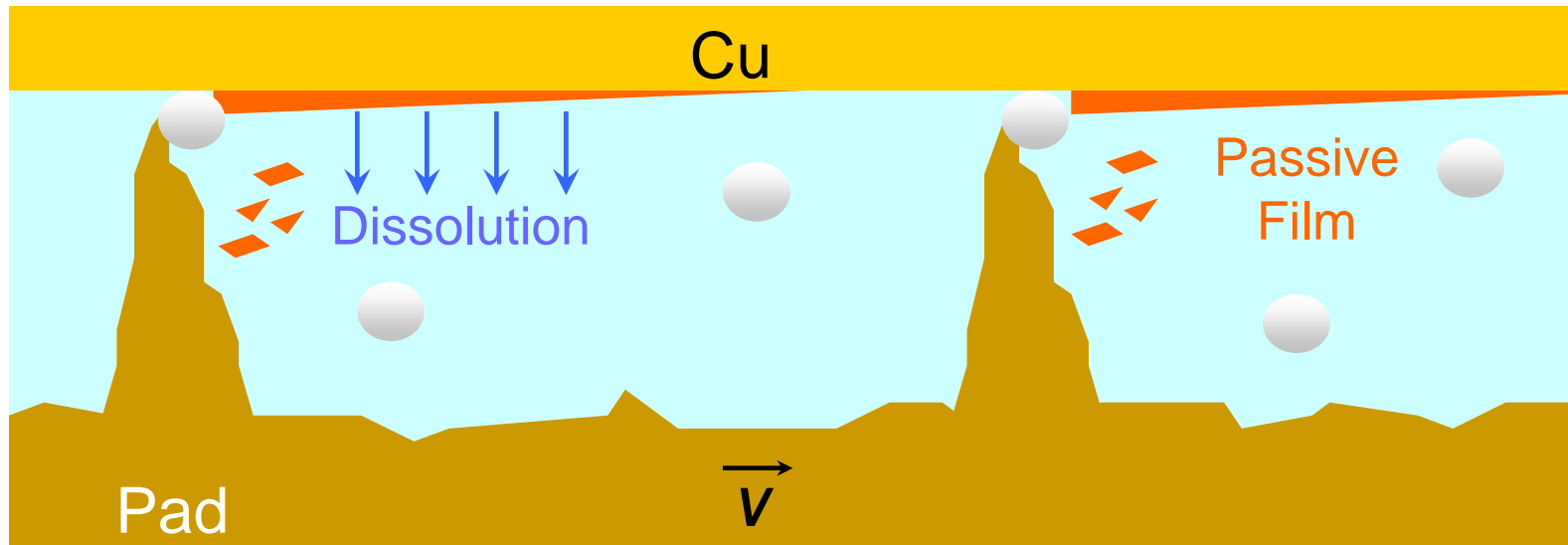
	Higher Rank = 1	Rank = 2	Lower Rank = 3
Removal Rate	Plus 20° Minus 20°	Plus 30° Zero	Minus 30°
Avg. Pad Leading Temperature	Plus 20°	Minus 20° Zero	Plus 30° Minus 30°

Results obtained with 95% confidence

Outline

- **Grooves Design (and experimental conditions)**
 - **Logarithmic-Spiral**
 - **Concentric Slanted**
- **Experimental Results**
 - **Logarithmic-Spiral**
 - **RR and average pad temperature**
 - **Average COF**
 - **Statistical comparison among different pad grooves**
 - **Concentric Slanted**
 - **RR and average pad temperature**
 - **Average COF**
 - **Statistical comparison among different pad grooves**
- **3-Step Model Development**
 - **Driving Force**
 - **Passive Film Formation and Dissolution**
- **3-Step Model Evaluation and Application**

3-Step RR Model



Passive Film Formation

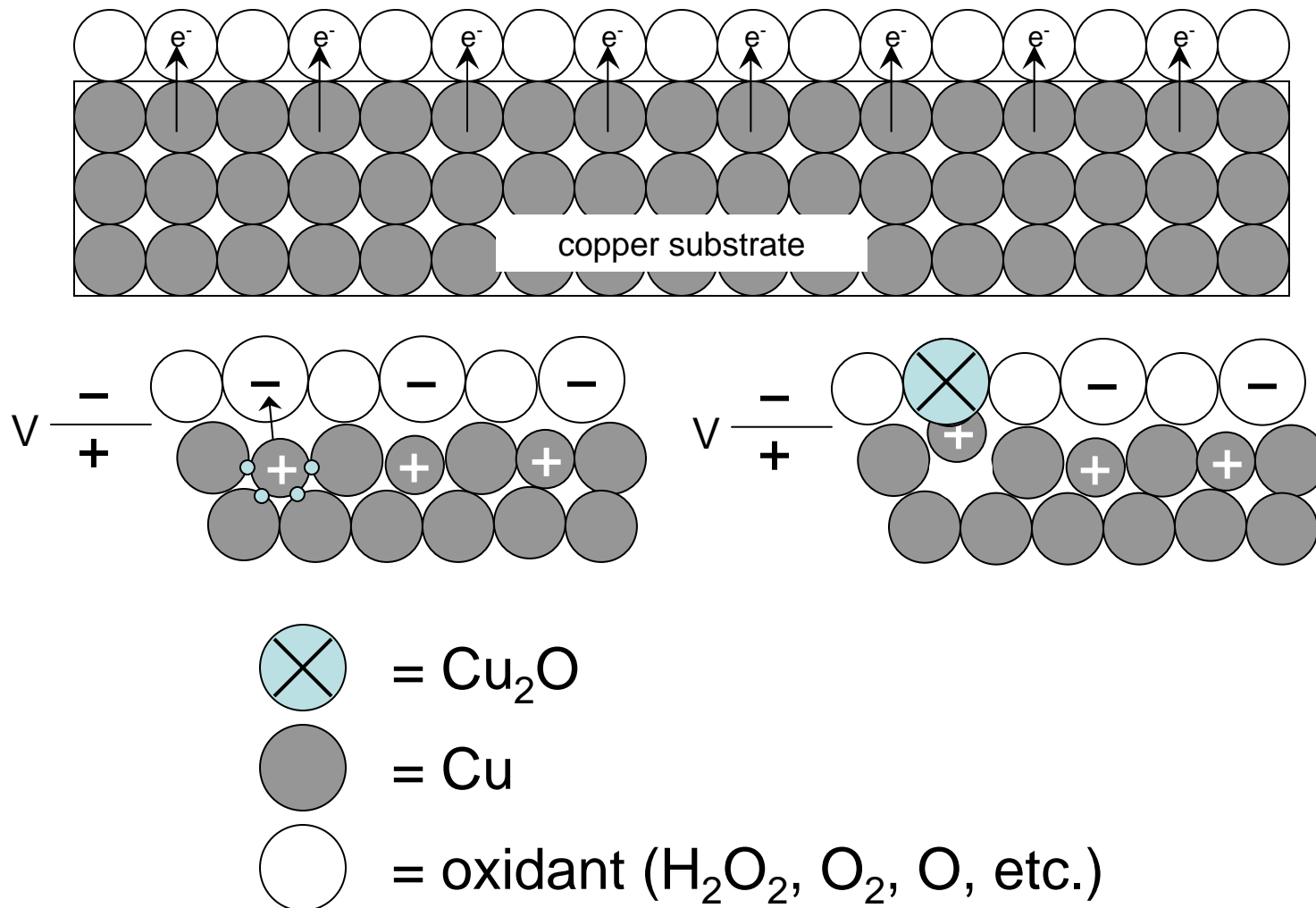
Mechanical Removal

Dissolution



$$RR = \frac{M_w}{\rho} \cdot \frac{k_1 \cdot (k_2 + k_3)}{k_1 + k_2 + k_3}$$

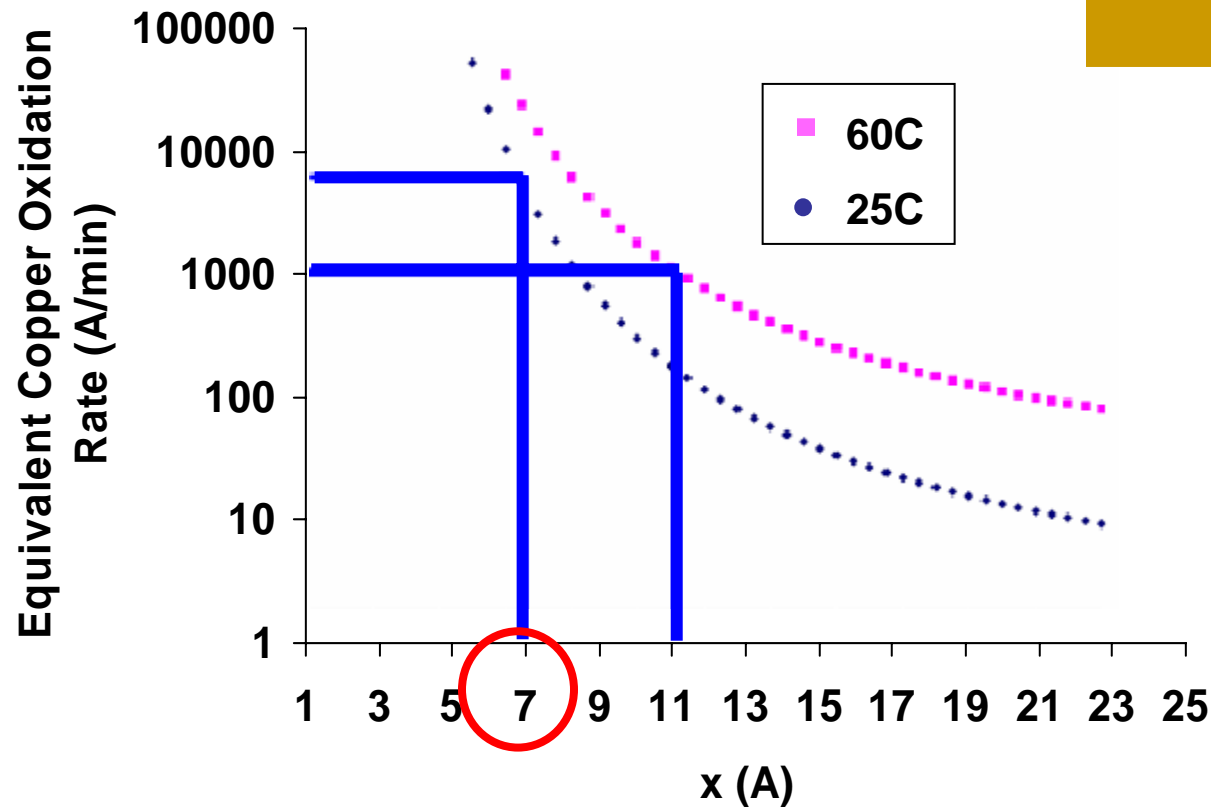
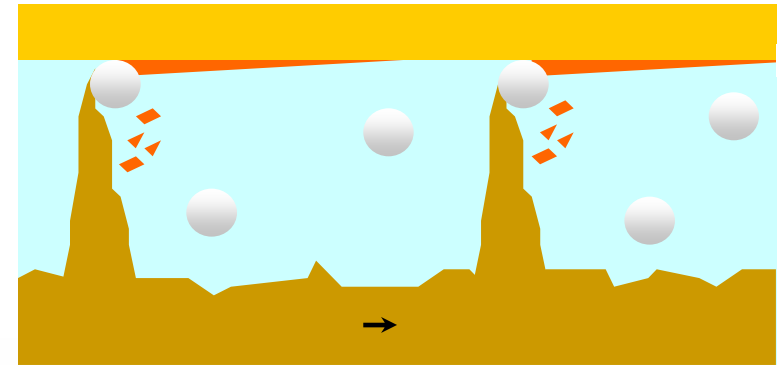
Copper Oxidation Mechanism



Incorporation into Proposed RR Model



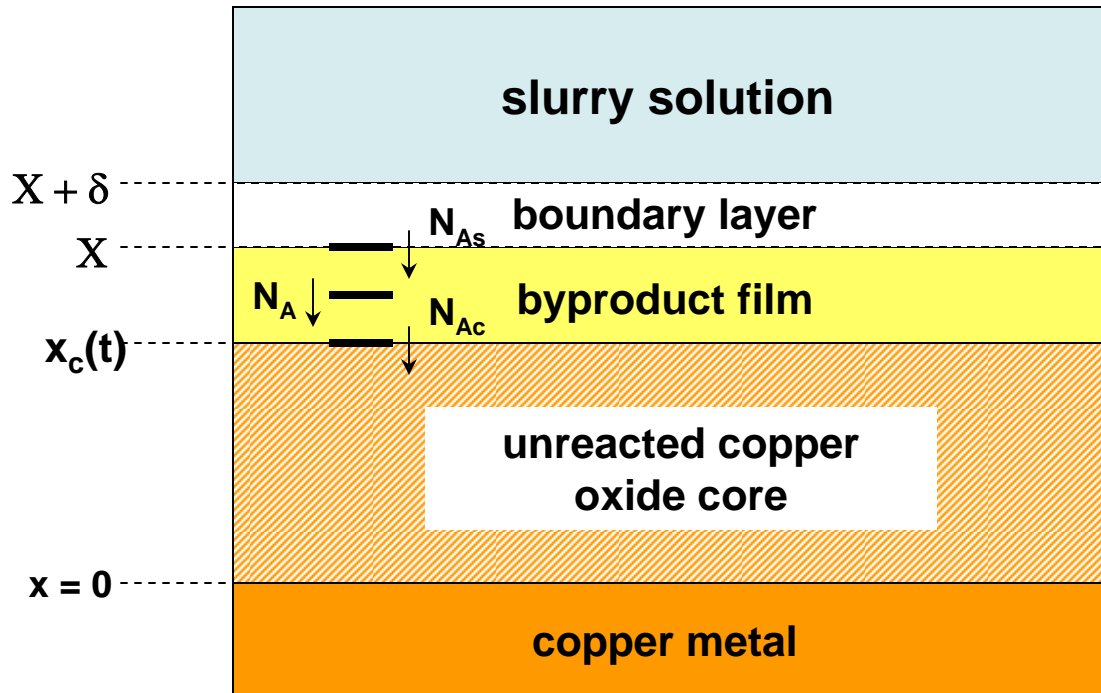
$$k_1 = \frac{\rho_{ox}}{Mw_{ox}} N\Omega f \exp\left(\frac{-W}{kT_w}\right) \exp\left(\frac{qa}{2kT_w x} V\right)$$



Typical Cu RR:
 1000 – 7000
 A/min

The characteristic
 oxide thickness
 used in this study is
 7 Å

Dissolution Process



- A soft byproduct film was observed on wafer surface
- Film was present after long times
- **Controlling Mechanisms**
 - Surface reaction
 - Linear profile
 - Diffusion through BL
 - Reported that profiles are not a function of stirring speed
 - Diffusion through the byproduct film

$$k_3 = \frac{-A \cdot \exp\left(-\frac{E_a}{R \cdot T_w}\right)}{(x_c - X)}$$

Mean Reaction and Flash Heating Temperature

Sorooshian et al., J. Tribology 127(3), pp. 461-468 (2005)

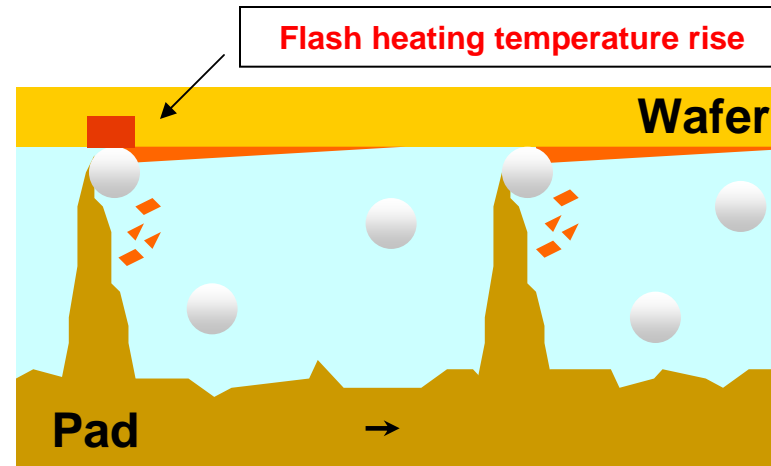
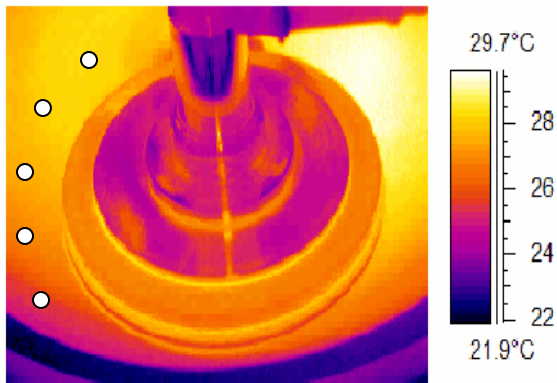
$$\bar{T}_w \approx \bar{T}_p + \Delta\bar{T}_f$$

\bar{T}_p = Mean leading edge pad temperature

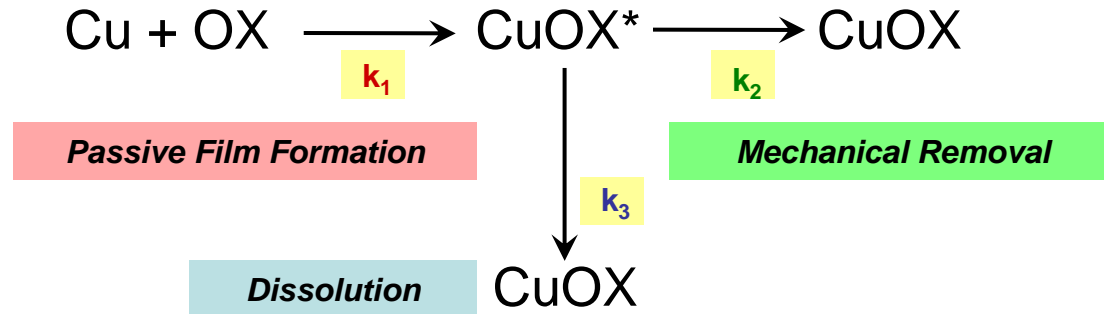
$\Delta\bar{T}_f$ = Mean flash increment

$$\Delta\bar{T}_f = \frac{\beta}{V^{1/2+e}} \cdot \mu_k \cdot (p \cdot V)$$

Mean leading edge pad temperature



Summary of 3-Step Model for Cu Removal



$$k_1 = \frac{\rho_{ox}}{M_{w_{ox}}} (N\Omega f) \exp\left(\frac{-W}{kT_w}\right) \exp\left(\frac{qa}{2kT_w x} V\right)$$

$$k_3 = \frac{-A \cdot \exp\left(-\frac{E_a}{R \cdot T_w}\right)}{(x_C - X)}$$

$$\Delta \bar{T}_f = \frac{\beta}{V^{1/2+e}} \mu_k \cdot (p \cdot V)$$

$$k_2 = c_p \mu_k \cdot (p \cdot V)$$

Real-time measurements can be used to predict RR

3 Fitting parameter

k_1 is characterized based on cation migration

Applicable at $p \cdot V = 0$ due to the addition of a dissolution step (k_3)

k_3 is characterized based on diffusion of complexant through by-product film

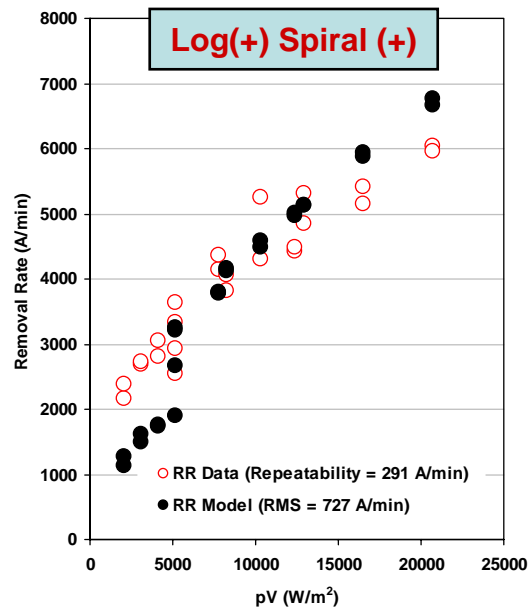
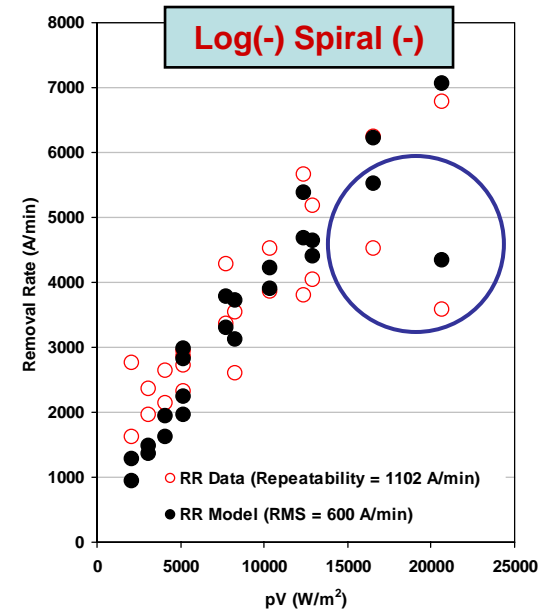
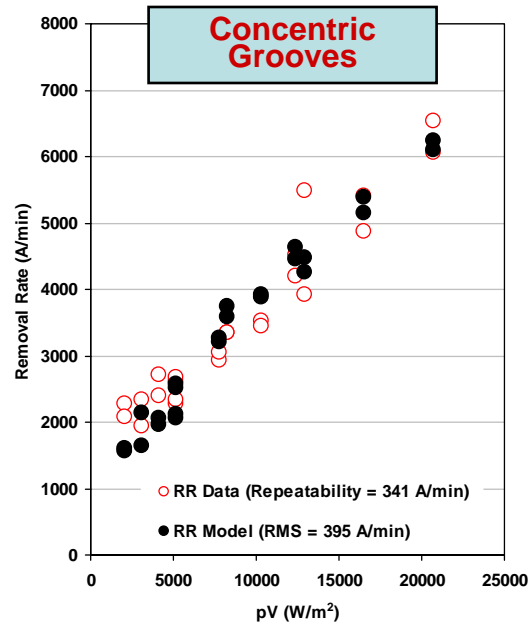
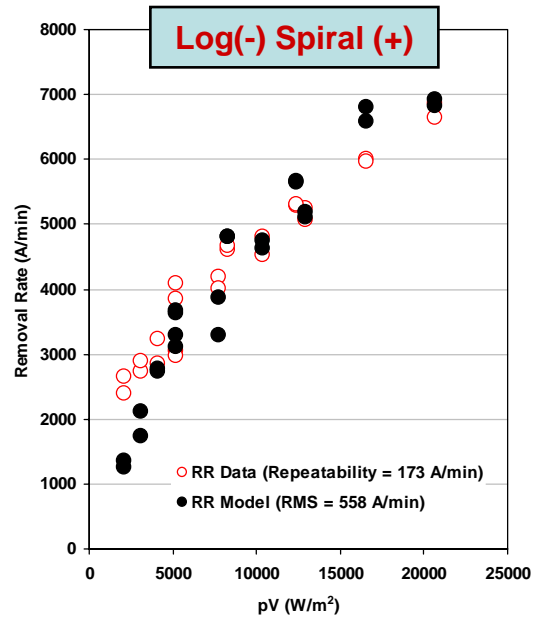
Dissolution rate (k_3) was found to be **negligible** for our system (**type of slurry, pressure and velocity conditions**)

However it becomes more important as **pressure x velocity** approaches zero

Outline

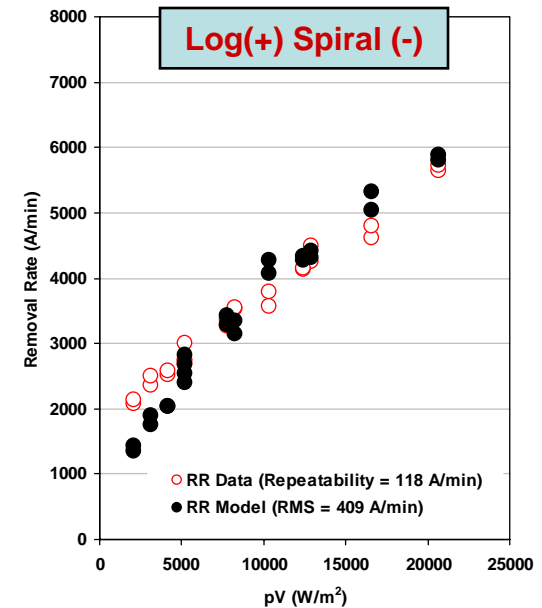
- **Grooves Design (and experimental conditions)**
 - **Logarithmic-Spiral**
 - **Concentric Slanted**
- **Experimental Results**
 - **Logarithmic-Spiral**
 - **RR and average pad temperature**
 - **Average COF**
 - **Statistical comparison among different pad grooves**
 - **Concentric Slanted**
 - **RR and average pad temperature**
 - **Average COF**
 - **Statistical comparison among different pad grooves**
- **3-Step Model Development**
 - **Driving Force**
 - **Passive Film Formation and Dissolution**
- **3-Step Model Evaluation and Application**

3-Step RR Model

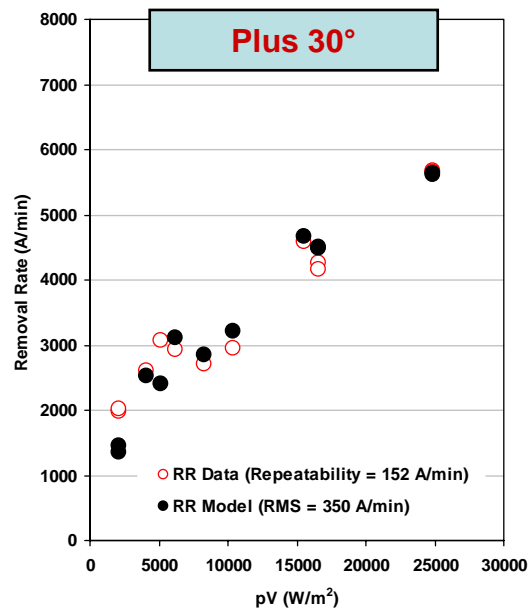
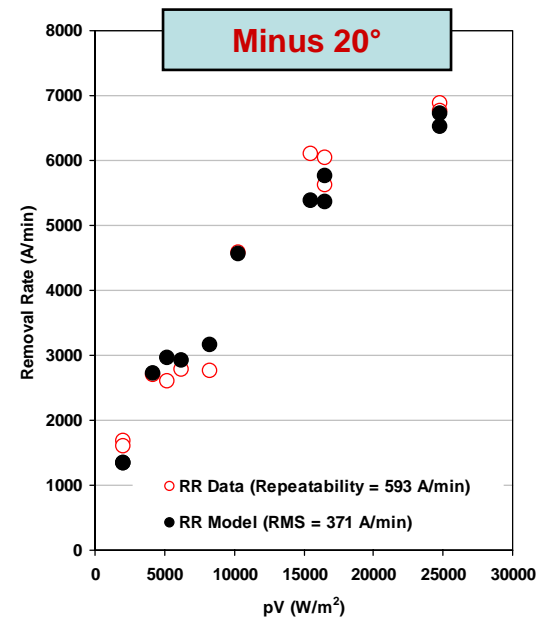
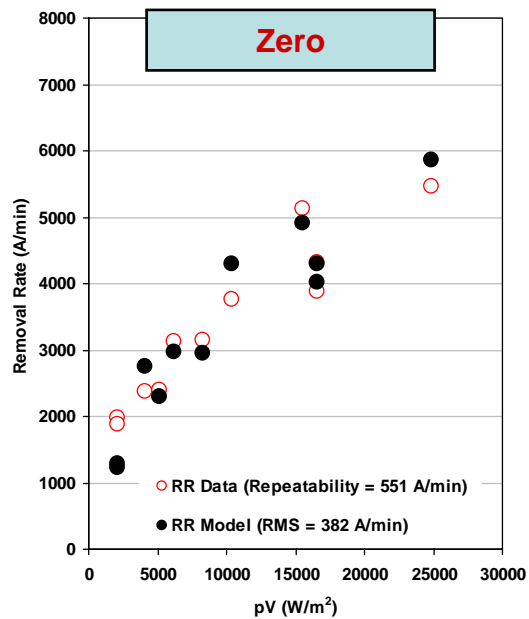
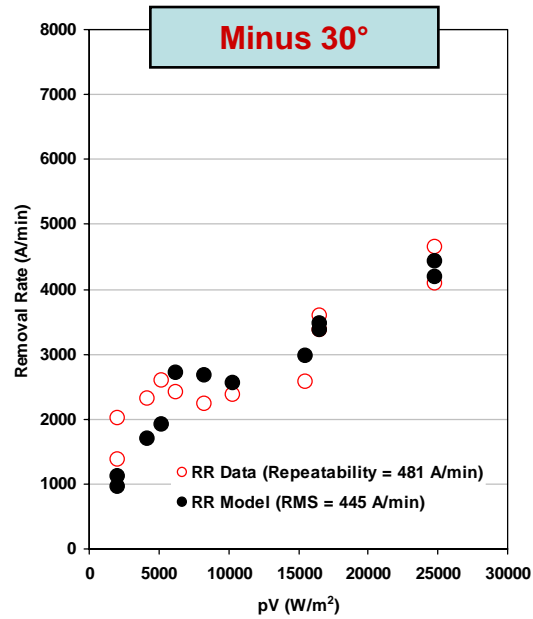


**Experimental
Repeatability range
120 – 1100 Å/min**

**Model RMS range
400 – 730 Å/min**

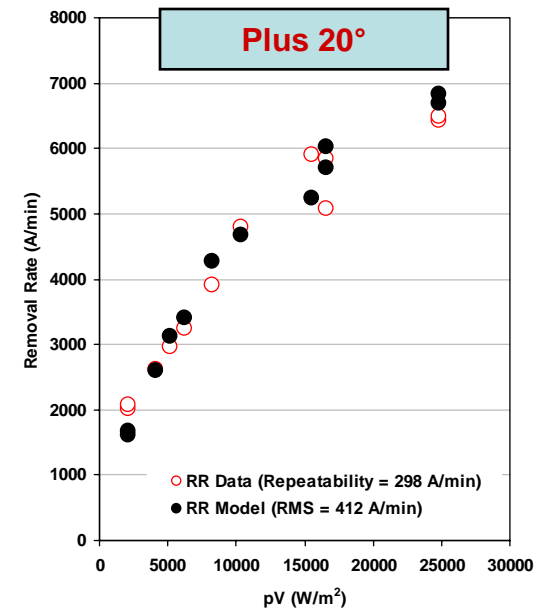


3-Step RR Model

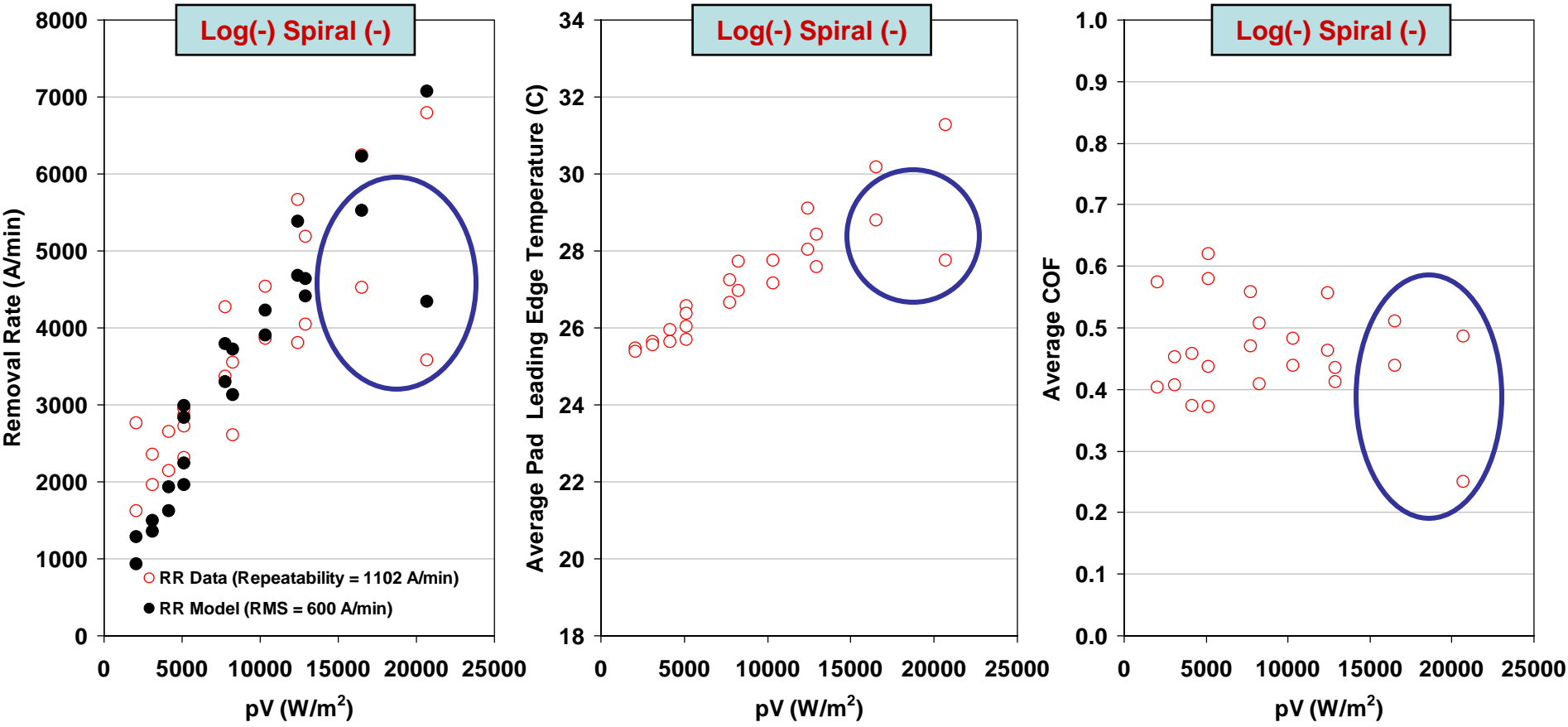


**Experimental
Repeatability range
150 – 590 Å/min**

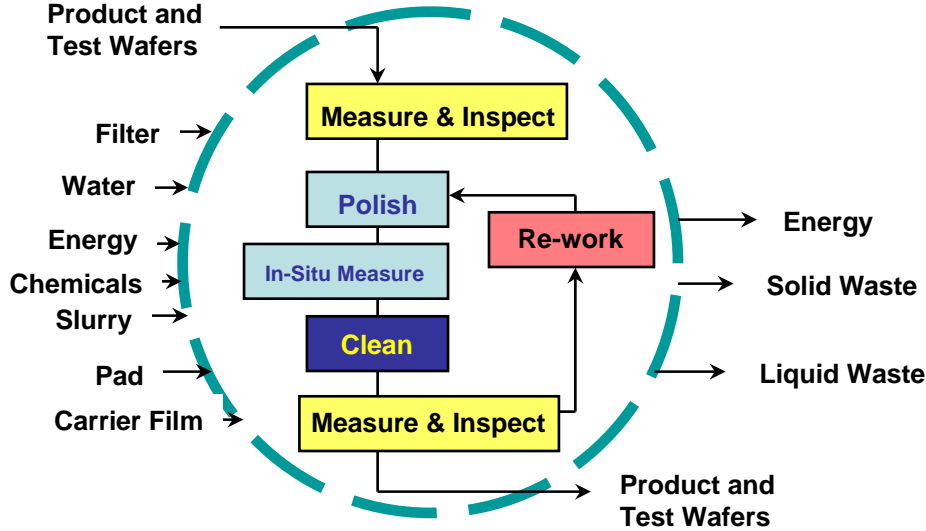
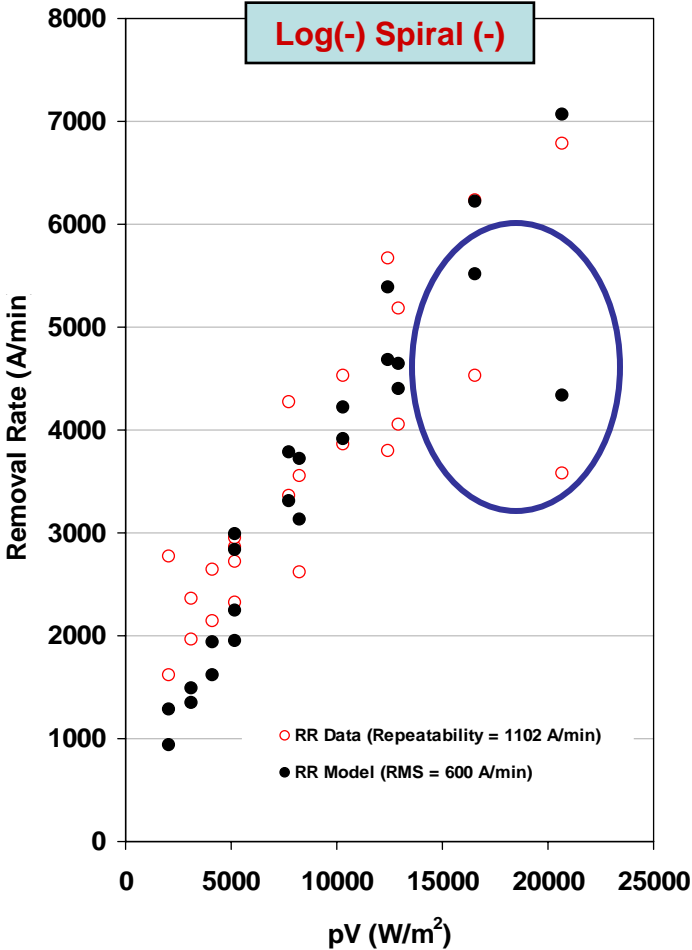
**Model RMS range
350 – 445 Å/min**



Applicability of 3-Step Model in Copper CMP

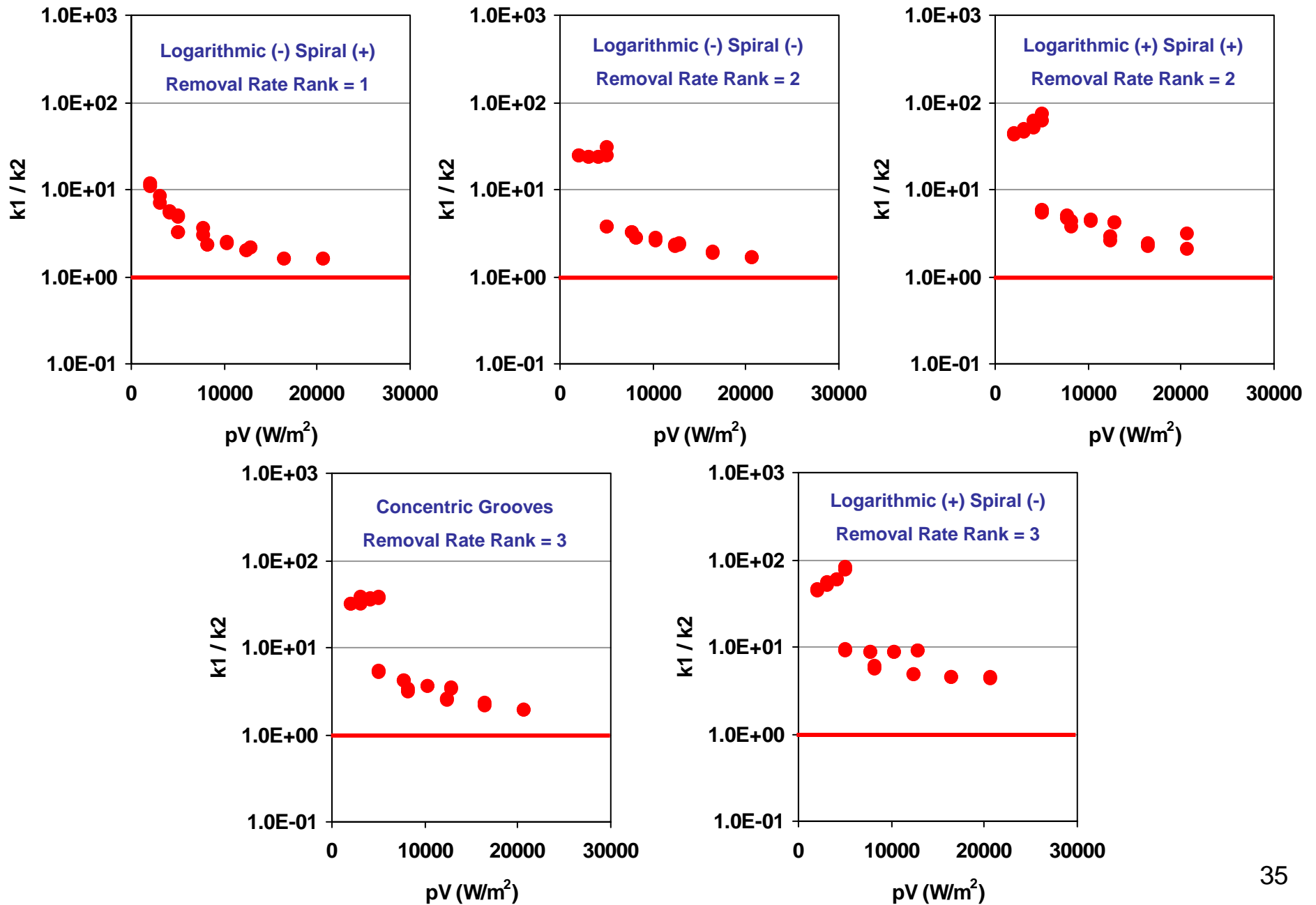


Applicability of 3-Step Model in Copper CMP

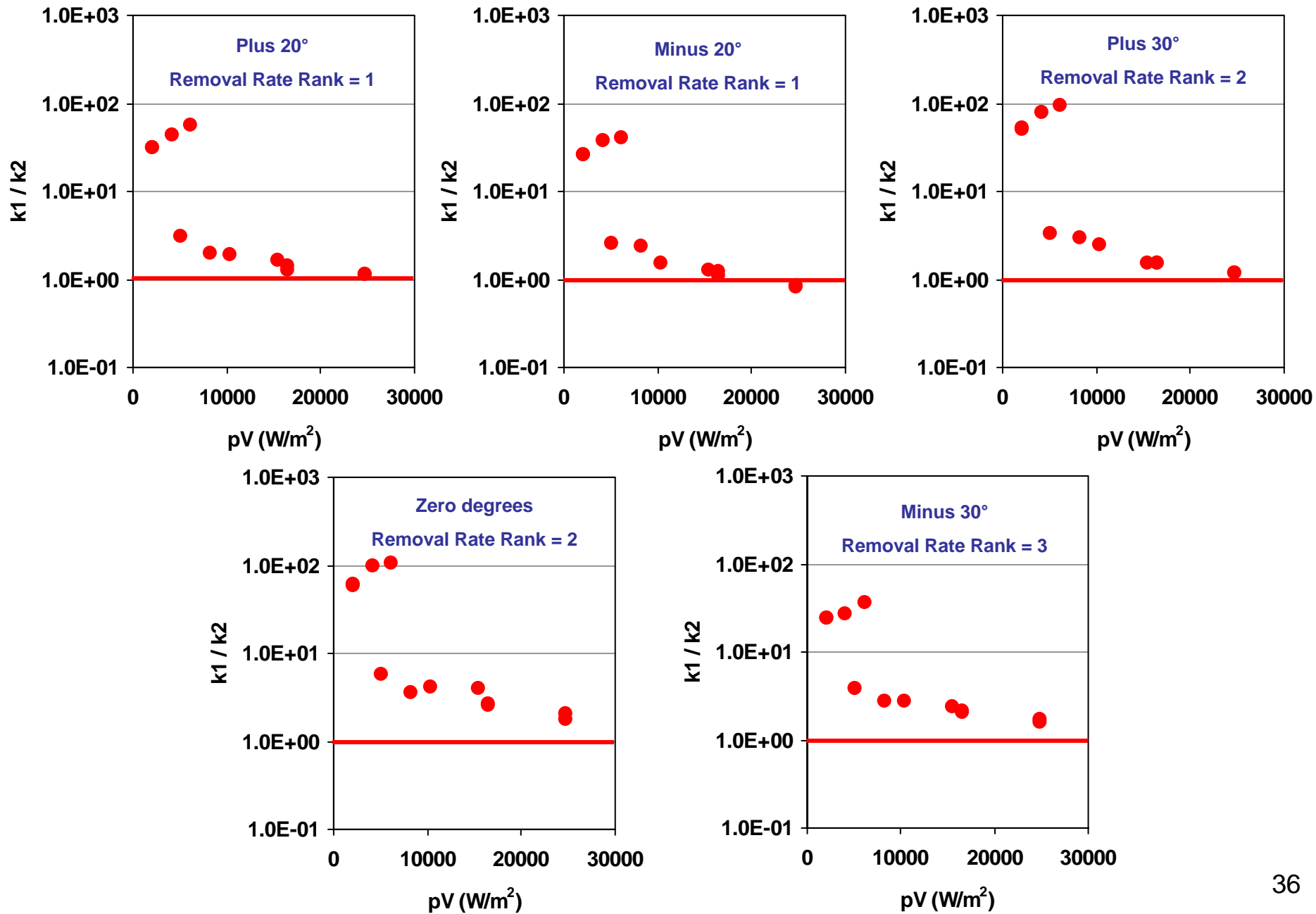


Prediction of process failure with in-situ measurement of temperature and COF

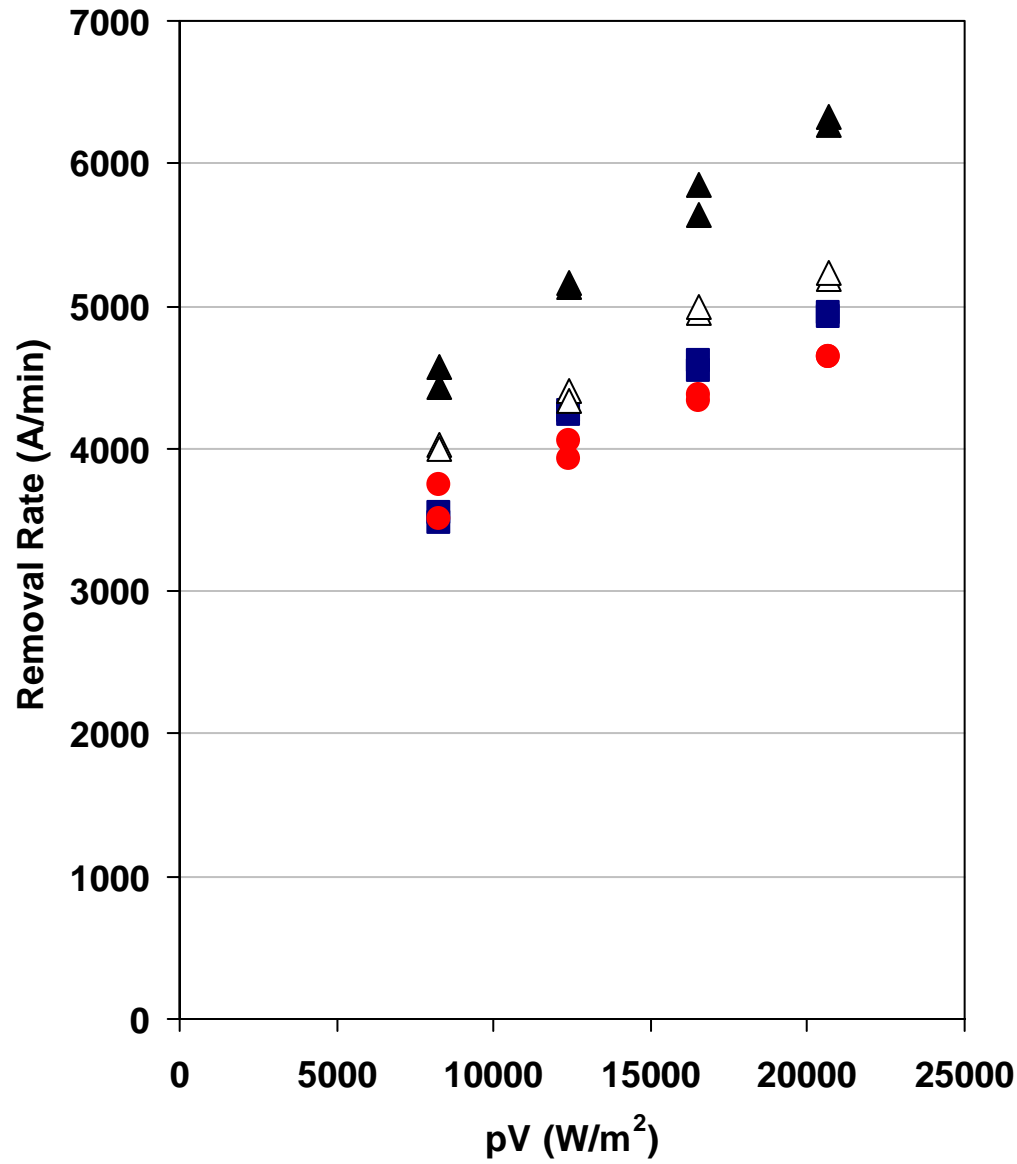
3-Step Model Rate Constants



3-Step Model Rate Constants



EHS Impact of Novel Groove Designs



- ▲ Log(-) Spiral(+) 110 cc/min (50% Reduction)
- △ Concentric grooves 110 cc/min (50% Reduction)
- Concentric grooves 165 cc/min (75% Reduction)
- Concentric grooves 220 cc/min

Preliminary results show significant reduction in slurry consumption

Removal rate increases slightly as slurry flow rate is decreased for the pad with concentric grooves

However, the Log(-) Spiral(+) pad results in much higher rates when slurry flow is reduced by 50%

Conclusions

- Novel groove design seems to be a good path to follow to obtain **higher removal rates at progressively smaller scales**
- Preliminary results show that these groove designs could **positively affect COO and EHS via decreasing pad and slurry consumption during copper CMP**
- **A novel 3-Step Model was presented**
 - Real-time measurements can be used to predict the removal rate of a wafer being polished
 - 3 Fitting parameter
 - k_1 is characterized based on cation migration
 - k_3 is characterized based on diffusion of complexant agent through by-product film
 - Applicable at $p \cdot V = 0$ due to the addition of a dissolution step (k_3)
- The 3-Step model predicts very well the behavior of the removal rate for different types of pads used in copper CMP. **The RMS falls in the range of 350 - 700 A/min whereas the repeatability range is 120 - 1200 A/min for all cases**

Conclusions

- The dissolution rate (i.e. k_3) does not play an important role for the system (**slurry type, pressure and velocity conditions**) evaluated in this study. However, this third step will become more and more significant as pV approaches zero
- The relative values of k_1 and k_2 as a function of pV shows that **the process is more limited by film removal through mechanical abrasion**, especially at low values of pV . However, **as pV increases this limitation is reduced** and there is a transition to a more balanced process
- The ratio of k_1/k_2 seems to indicate that as pV increases, the **faster** each pad (groove design) approaches **balance between film growth and film removal**, the **higher the removal rate** for that pad (i.e. groove design)

Future Work

- **Perform rigorous analysis and modeling of the effect of groove design (i.e. Logarithmic-Spiral) under reduced slurry flow rates**
- **Perform Dual Emission UV Enhanced Fluorescence (DEUVEF) analysis to evaluate the effect of pads with slanted groove patterns on slurry flow**
- **Expand the 3-step copper removal model by characterizing the dependence of copper oxide film growth on sliding velocity and conditioning process**

Acknowledgements

- **Ara Philipossian (UA)**
- **Darren DeNardis (Intel)**
- **Len Borucki (Araca)**
- **Duane Boning (MIT)**
- **Engineering Research Center for Environmentally Benign Semiconductor Manufacturing**
- **Tasutoshi Suzuki (Toho Engineering)**
- **Fujimi Incorporated**